Biochimica et Biophysica Acta 1840 (2014) 219–244

Contents lists available at ScienceDirect

Biochimica et Biophysica Acta

journal homepage: www.elsevier.com/locate/bbagen

Berberine and S allyl cysteine mediated amelioration of DEN + CCl4 induced hepatocarcinoma

Dipanwita Sengupta, Kaustav Dutta Chowdhury, Avik Sarkar, Soumosish Paul, Gobinda Chandra Sadhukhan *

Molecular Biology and Tissue Culture Laboratory, Post Graduate Department of Zoology, Vidyasagar College, Kolkata-700006, India

ARTICLE INFO

Article history:
Received 21 December 2012
Received in revised form 14 August 2013
Accepted 26 August 2013
Available online 31 August 2013

Keywords:
S allyl cysteine
Berberine
p53 acetylation
Di ethyl nitrosamine
Carbon tetrachloride
Oxidative stress

ABSTRACT

Background: Diethylnitrosamine (DEN) and carbon tetrachloride (CCl4) have been used as initiator and promoter respectively to establish an animal model for investigating molecular events appear to be involved in development of liver cancer. Use of herbal medicine in therapeutics to avoid the recurrence of hepatocarcinoma has already generated considerable interest among oncologists. In this context studies involving S-allyl-cysteine (SAC) and berberine have come up with promising results. Here we have determined the individual effect of SAC and berberine on the biomolecules associated with DEN + CCl4 induced hepatocarcinoma. Effective therapeutic value of combined treatment has also been estimated.

Methods: ROS accumulation was analyzed by FACS following DCFDA incubation. Bcl2-Bax and HDAC1-pMdm2 interaction were demonstrated by co-immunoprecipitation. Immunosorbent assay was performed to analyze PP2A and caspase3 activities. MMP was determined cytofluorimetrically by investigating JC-1 fluorescence. AnnexinV binding was demonstrated by labeling the cells with AnV-FITC followed by flow cytometry.

Results: CytochromeP4502E1 mediated bioactivation of DEN + CCl4 induced Akt dependent pMdm2-HDAC1 interaction that led to p53 deacetylation, probable cause of its degradation. In parallel, oxidative stress dependent Nrf2-HO1 activation increased Bcl2 expression which in turn stimulated cell proliferation. SAC in combination with berberine inhibited Akt mediated cell proliferation. Activation of PP2A as well as inhibition of JNK resulted in induction of apoptosis after 30 days of treatment. Extension of combined treatment reverted tissue physiology towards control. Co-treated group displayed normal tissue structure.

Conclusion and general significance: SAC and berberine mediated HDAC1/Akt inhibition implicates the efficacy of combined treatment in the amelioration of DEN + CCl4 induced hepatocarcinoma.

1. Introduction

Hepatocellular carcinoma (HCC) is the 5th common cancer in the world. It is one of the most frequent solid tumor generating cancers that kills almost half-million people around the world each year [1,2]. Though a great improvement has been done in understanding of the molecular mechanisms involved in the regulation of hepatocarcinogenesis [3,4], many of the underlying mechanisms still remain unexplored.

Clinical study suggests that surgery is the treatment of choice for HCC. It is the removal of the tumor and is likely to be the most successful disease-directed treatment [4,5]. Radiation therapy is another way of treatment where high-energy X-rays are used to kill cancer cells [6,7]. Both surgery and radiation therapy end up with chemotherapy to prevent recurrence of carcinogenesis in the long run [8,9]. Also it remains the standard of care for HCC either as a first-line treatment or as an adjuvant [9,10]. During this treatment chemo-drugs are used to kill cancer cells usually by stopping the cancer cells' ability to grow and divide [11,12].

According to reports chemotherapy with cytotoxic agents such as doxorubicin, cisplatin or 5-fluorouracil, shows low response rate (<10%) without a clear benefit in overall survival [8,13]. This type of therapy is poorly tolerated in the patients due to systemic toxicities and side effects [9,14]. Considering these scenarios, chemo-drugs may be used in lower dose but the safety of the lower dosages and the efficacy of the higher dosages is a never-ending balancing act. A minimal dosage of the drugs gives a better safety profile while the higher dosages typically give better efficacy [13,15].

Abbreviations: ROS, reactive oxygen species; FACS, fluorescence activated cell sorter; DCFDA, 2′,7′-Dichlorofluorescein diacetate, TCA, tri choloro-acetic acid; HDAC1, histone deacetylase type1; pMdm2, phosphorylated Mdm2; PP2A, protein phosphatase 2A; MMP, mitochondrial membrane potential; FITC, fluorochrome iso-thiocyanate; Nrf2, nuclear factor erythroid 2 related factor 2; HO1, hemoxygenase1; JNK, c-Jun N terminal kinase; CYP2E1, cytochromeP4502E1; DTNB, 5,5-dithiobis (2 nitrobenzoic acid); GR, glutathione reductase; NADPH, nicotinamide adenine dinucleotide 2′-phosphate reduced; SOD, superoxide dismutase; NaCN, sodium cyanide; PCNA, proliferating cell nuclear antigen; BSA, bovine serum albumin; NBT/BCIP, nitro blue tetrazolium/5-bromo-4-chloro-3-indolyl phosphate; PT, co-treated group; POT, post treated group; S, SAC treated group; B, berberine treated group; S + B, treatment with combination of SAC and berberine;NS, Non significant

* Correspondence author at: Department of Zoology 39, Sankar Ghosh Lane, Kolkata 700006, India. Tel.: +91 33 9433236599.
E-mail address: sadhukhan.g.c@gmail.com (G.C. Sadhukhan).

0304-4165/$ – see front matter © 2013 Elsevier B.V. All rights reserved.
http://dx.doi.org/10.1016/j.bbagen.2013.08.020

For this reason targeted therapy is an upcoming treatment that targets the cancer's specific genes, proteins, or the tissue environment that contributes to cancerous growth, proliferation and survival [10,12]. Currently to differentiate cancerous cell from healthy ones, immunotherapy is designed through potentiating antigen-specific immune responses induced by synthetic vaccine to fight against liver cancer [16]. Nano-delivery of drugs may be considered as another promisable therapeutics where magnetically vectored nanoparticles act as vehicles for the site-specific delivery of drugs [17]. These treatments are costly and require more phase III trials for validation of their activities [18,19]. Thus alternative tissue targeted therapeutics needs to be proposed for the effective amelioration of liver cell carcinoma.

In the pursuit of such alternative therapeutics mice were exposed to diethylnitrosamine and carbon tetrachloride (DEN + CCl4) to develop a model which is frequently used to investigate different stages of hepatocarcinoma [20]. Protective effects of S-allyl cysteine (SAC; an organosulphur isolated from garlic extract) on the temporal patterns of tumor marker enzymes in DEN-induced hepatocarcinogenesis have been studied elsewhere [21,22]. The efficacy of berberine (an isoquinoline alkaloid present in *Berberis* sp., *Hydrastis canadensis*, *Phellodendron amurense*, *Coptis chinensis*, *Tinospora cordifolia* and to a smaller extent in *Argemone mexicana* and *Eschscholzia californica*) to inhibit chemical carcinogenesis is also reported [23,24]. Here we have investigated whether SAC and berberine treatment can be considered as an effective tissue targeted HCC therapy. Furthermore, we have identified the signaling molecules responsible for carcinogenic amelioration during SAC + berberine treatment. These classified molecules can be regarded as centre molecules during designing of the future therapeutics in other forms of HCC.

2. Materials and methods

2.1. Materials

Rabbit anti-Bcl2 (phospho S70), anti-CYP2E1 and anti-PP2A polyclonal antibody were obtained from Abcam Inc. MA, USA. Rabbit polyclonal anti HDAC1 antibody was acquired from Biovision Inc. CA, USA. Rabbit polyclonal anti phospho-MDM2 (Ser166) antibody and anti acetyl-p53 (Lys379) antibody were bought from Cell Signaling Technology, Inc., MA, USA. Rabbit polyclonal anti-PCNA, anti-cyclinD1, anti-Bcl2, anti-Bax, anti-pJNK, anti-p53, anti-pAkt (pSer473 and pThr308 pAkt), anti Mdm2, anti-Akt, anti-p17caspase3, anti-HO1, anti-Nrf2, anti-cytochrome C, goat antirabbit IgG-AP, rabbit polyclonal anti-β actin antibody were bought from Santa Cruze Biotechnology, CA, USA. HDAC1 assay kit was procured from Cayman Chemical Company, MI, USA. DuoSet® IC Human/Mouse/Rat Active PP2A assay kit and Quantikine Rat/Mouse Cytochrome C Immunoassay kit were obtained from R&D Systems, Inc. MN, USA. Nitrocellulose membrane was obtained from Millipore Corporation, MA, USA. DCFDA, 2′,7′-Dichlorofluorescein diacetate and Protease inhibitor cocktail, set III, (EDTA free) were purchased from Calbiochem, NJ, USA. Caspase3 Substrate DEVD-pNA was bought from Biovision Inc., CA, USA. Annexin V-FITC apoptosis detection kit was acquired from BD Pharmingen, CA, USA. High-density media Percoll was purchased from Pharmacia, Uppsala, Sweden. Mitochondria isolation kit, protein A-sepharose4B, β-nicotinamide adenine dinucleotide 2′-phosphate reduced tetrasodium salt hydrate (β-NADPH), Triton X-100, diethyl nitrosamine, carbon tetrachloride, S-allyl-L-cysteine, berberine chloride, collagenase type IV, trypan blue, D-mannitol, L-glutathione reduced, glutathione reductase, meta-phosphoric acid, 5,5′-dithiobis(2-nitrobenzoic acid), N-ethylmaleimide, pyrogallol, catalase, sodium cyanide, N,N,N′,N′-tetramethylethylenediamine, Triton™ X-100, 4-nitrocatechol sulfate dipotassium salt, 4-nitrophenol trichloroacetic acid, 2-thiobarbituric acid, ethylene glycol-bis(2-aminoethylether)-N,N,N′,N′-tetraacetic acid (EGTA), Hanks' balanced salt solution, hydrogen peroxide, hemin, glucose, D-glucose 6-phosphate sodium salt, glucose-6-phosphate dehydrogenase, rhodamine 123, paraformaldehyde, nitro blue tetrazolium/5-bromo-4-chloro-3-indolyl phosphate (SIGMAFAST™ BCIP®/NBT) ready mix tablet, diaminobenzidine (DAB) and all other fine chemicals (unless mentioned) were purchased from Sigma-Aldrich Corporation, St.Louis, MO, USA. ALT, AST, LDH and ALKP measurement kits were obtained from TECO Diagnostics, CA, USA.

2.2. Animals

Animal experiments were carried out in male swiss albino mice (4-6 weeks old; 25-30 g). They were bred in-house and maintained at 27 ± 2 °C with relative humidity of 44–56% and 12 h light/darkness cycle as well as free access of food and water in a cross-ventilated room. Ethical guidelines of animal ethics committee of Vidyasagar College, University of Calcutta on handling and use of experimental animals were followed during the conduct of the study. Experiments were designed to minimize animal suffering and to use the minimum number associated with valid statistical evaluation.

2.3. Carcinogen exposure and drug treatment

Before commencement of experiments animals of both control and experimental groups were kept separately under standard controlled condition and food was withdrawn for 12 h with free access to water. Mice were exposed to DEN (as a hepatocarcinoma initiator) at 100 μg/l/day in drinking water and CCl4 (as a hepatocarcinoma promoter) at a dose of 100 mg/kg body weight in olive oil for 90 days. Animals received olive oil by oral feeding in the respective control groups. For the co-treatment in parallel to DEN + CCl4 exposure respective groups of mice were gavaged with 8 mg/kg body weight berberine, 250 mg/kg body weight SAC or SAC + berberine in combination. While in the post treatment after 90 days exposure of DEN + CCl4 animals were treated with berberine; SAC or combined drug for 60 days. A group of mice were sacrificed after 90 days of DEN + CCl4 exposure and also from co-treated group for experimental analysis. To study the effect of post treatment another group of animals were sacrificed after 30 days. Finally treatment schedule was ended after 60 days of drug treatment and mice were euthanized following a gap of 10 days after receiving the last dose of drug. In the treated group animals received SAC orally, daily, in doses 60, 120, 250 and 350 mg/kg body weight and berberine at the doses of 2, 4, 8 and 12 mg/kg body weight. Drug treated DEN + CCl4 exposed mice were grouped according to the dose of drug treatment with 4 animals in each group. Untreated carcinogen exposed animals received an equal amount of distilled water (vehicle) by oral feeding.

90 days of DEN + CCl4 exposed mice were injected 50 mg/kg body weight SP600125, the potential JNK inhibitor, five times per week for 30 days. Another group of carcinogen exposed mice were treated with okadaic acid at a dose of 150 μg/kg body weight by gavage for seven days.

To study the effect of antioxidants DEN + CCl4 exposed mice were treated with different antioxidant inhibitors. One group of mice was gavaged with 2 methoxyestradiol, the potential MnSOD inhibitor, with a dose of 60 mg/kg body weight for 4 weeks. Diethyldithiocarbamate, the Cu Zn SOD inhibitor, was administered i.p. at a dose of 50 μmol/kg body weight on alternate days and the total treatment period was 21 days. Another group of mice were treated with 500 mg/kg body weight/day L-Buthionine sulfoximine, the γ-glutamylcysteine synthetase inhibitor, for 14 days. 3-amino-1,2,4-triazole (AT), a specific catalase inhibitor, was injected intraperitoneally at a dose of 0.5 g/kg body weight for 7 days. Zinc protoporphyrin IX was injected intraperitoneally weekly four times for 4 weeks.

2.4. Toxicity study and effective dose determination

Blood was collected from control, carcinogen exposed and drug treated animals in non-heparinized tubes for serum separation. The

activity of alanine transaminase (ALT), aspartate transaminase (AST), serum alkaline phosphatase and serum lactate dehydrogenase were determined spectrophotometrically according to standard procedures using a commercially available diagnostic laboratory kit. Activity of those stress specific enzymes were normalized against their respective control values and used as markers for toxicity study and effective dose determination.

2.5. Isolation of hepatocytes

Hepatocytes were isolated following standard two step collagenase perfusion technique [25]. During this procedure at first liver was taken out after dissecting the surrounding structures and perfused in a recirculating system at 30 ml/min for 3 min with Hanks'-bicarbonate buffer containing 0.6 mM EGTA. The liver was then perfused in a recirculating system with Hanks'-bicarbonate buffer containing 3 mM calcium chloride and 60–100 mg standard collagenase (Sigma L blend) for up to 10 min. After disruption of the liver capsule digested liver parenchyma remained suspended in the Hanks' buffer. Resulting cell suspension was filtered and washed at 400 g for 3 min. Cell viability was determined by Trypan blue exclusion.

2.6. Isolation of microsomal, mitochondrial, nuclear and cytosolic fraction

Mice were killed by cervical dislocation, and the liver was immediately removed and chopped into fine pieces, washed with 0.25 M sucrose and homogenized using an isolation buffer consisted of 210 mM mannitol, 70 mM sucrose, 2 mM Hepes, pH 7.4, and 0.05% BSA. The homogenate was centrifuged at 800 *g* for 8 min, the pellet was removed, and the centrifugation process was repeated. Supernatant was then centrifuged at 8,000 *g* for 10 min, the pellet was washed with the isolation buffer, and the centrifugation was repeated. Isolated microsomal pellet was resuspended in buffer (pH 7.4) and stored at -80 °C for experimental purpose [26].

For the purification of mitochondria, microsomal pellet were further fractionated by centrifugation at 8,500 *g* for 10 min in Percoll gradient consisted of three layers of 18%, 30%, and 60% (w/v) Percoll in sucrose-Tris buffer (0.25 M sucrose,1 mM EDTA, and 50 mM Tris), pH 7.4. Mitochondria were collected from the interface of 30% and 60% Percoll, washed with the sucrose-Tris buffer and stored at -80 °C for future studies [26,27]. Isolated fraction was blotted against anti β actin antibody to confirm that it was successfully separated from cytosolic fraction.

Nuclear extract formation was initiated after homogenization with isolation buffer and the produced homogenate was centrifuged for 10 min at 2000 *g* to pellet nuclei. Pellet obtained from this low speed centrifugation was subjected to a second centrifugation for 20 min at 25,000 *g* to remove residual cytoplasmic material and this pellet was designated as crude nuclei. These crude nuclei were resuspended and homogenized in a buffer containing 20 mM HEPES (pH 7.9), 25% (v/v) glycerol, 0.42 M NaCl, 1.5 mM $MgCl_2$, 0.2 mM EDTA, 0.5 mM phenylmethylsulfonyl fluoride (PMSF) and 0.5 mM DTT (dithiothreitol). The suspension was stirred gently for 30 min and then centrifuged for 30 min at 25,000 *g*. The supernatant was dialyzed against the dialysis buffer for 2 h and was centrifuged at 25,000 *g* for 20 min. Resulting precipitate was discarded and supernatant was designated as nuclear extract which was frozen in aliquots in liquid nitrogen and stored at -80° [28]. Isolated fraction was blotted against anti β actin antibody to confirm that it was successfully separated from cytosolic fraction.

Cytosolic fraction was isolated after suspending the cells in buffer (50 mM Tris–HCl, pH 7.5,100 mM NaCl, 10 mM EDTA and 2.5%, v/v Triton-X 100) containing 1/1000 (v/v) protease inhibitor cocktail and was sonicated four times (15 s each time) for total lysis. Sonicated extract was centrifuged at 10,000 *g* for 10 min and the supernatant containing cytosolic fraction was stored at −20 °C until use [29]. Isolated fraction was blotted against anti laminB antibody and anti VDAC1/porin antibodies to confirm that it was successfully separated from nuclear and mitochondrial extract.

2.7. Measurement of Cytochrome P450 2E1 (CYP2E1) activity

CYP2E1 activity in liver microsomes was determined by monitoring the formation of para-nitro-catechol from para-nitro-phenol following the method of Chang et al. [30]. Isolated microsomal protein was added to the assay buffer containing 50 mM potassium phosphate, pH 7.4, 10 μl of 5 mM para-nitro phenol and 1 mM NADPH to initiate enzymatic reaction. Reaction mixture was then incubated at 37 °C for 30 min in a water bath. After incubation 100 μl of 20% (v/v) TCA was added to stop the enzymatic reaction. Next reaction mixture was centrifuged at 10,000 *g* for 5 min and supernatants were transferred to a clean test tube containing 2 M NaOH for neutralization. Enzymatic product para-nitro-catechol was quantified spectrophotometrically (UV-1240 Pharma Spec, Shimadzu) by measuring the absorbance at 535 nm.

2.8. Estimation of intracellular ROS

Accumulation of intracellular ROS was determined by incubating 5% cell suspension with 5 μM 2,7-dichlorofluorescein diacetate (DCFDA) at 37 °C for 15 min. Cells were washed with PBS buffer pH 7.4 to remove excess probe. Oxidation of fluorescent probe DCFDA to dichlorofluorescin (DCF) was determined cytofluorimetrically in FACS Calibur (BD Biosciences, Mountain. View, CA, USA) equipped with an argon laser lamp (ex: 488 nm) according to the method of Kim et al. [31]. The mean cell fluorescence values were expressed as histogram.

2.9. Immuno blot analysis

Whole cell lysates for PCNA, CyclinD1, Bcl2, Bax, pJNK, p53, Mdm2, pMdm2, pAkt, Akt and caspase-3 p17 antibody; microsomal fraction for CYP2E1, HO1; cytosolic fraction for Nrf2, cytochrome C while nuclear fraction for Nrf2, nuclear p53, acetyl-p53 were run on SDS-PAGE. Resolved proteins were transferred to nitocellulose membrane. Then the membrane was blocked in 3% BSA in TBST (50 mmol/L Tris-HCl, pH 7.5, 150 mmol/L NaCl, 0.1% Tween20) and subsequently incubated with respective primary antibody (1:500 to 1:1000 dilutions in TBST). Next membrane was incubated with alkaline phosphatase or HRP conjugated secondary antibody (1:2000 dilutions in TBST) and binding signals were visualized with NBT-BCIP or TNB substrate as required. Respective band densitometric analysis was performed with ImageJ software (NIH, Bethesda, MD, USA). Anti-β-actin and anti laminB were used as an internal loading control.

Bcl2 present in the cell lysate was immunoprecipitated as described by May et al. [32]. Briefly, whole cell lysates were incubated with anti-Bcl2 antibody for overnight at 4 °C and were then incubated with protein A-sepharose 4B for 2 h at 4 °C. Antigen–antibody complexes were separated from the protein A-sepharose beads with 100 μl of SDS-sample buffer, boiled for 5 min, and resolved by SDS-PAGE. Immunoprecipitates were blotted using antibody against Ser70 phosphorylated Bcl2 or Bax as primary antibody and ALKP conjugated anti rabbit as secondary antibody. Developed bands demonstrated the status of Bcl2 phosphorylation and Bcl2:Bax interaction respectively after employing the conventional NBT/BCIP chromogenic stain. Levels of Bcl2 in the precipitated samples were also estimated following the standard protocol.

Co-immunoprecipitation of pMdm2 with HDAC1 was conducted by incubating nuclear extract with anti-HDAC1 antibody [33] and immune complexes were precipitated with protein A-sepharose 4B. Imunoprecipitated pMdm2 were analysed by SDS-PAGE. Immuno blotting with the anti-pMdm2 Ser166 as primary and ALKP conjugated anti rabbit as secondary antibody displayed HDAC1-pMdm2 interaction after staining with NBT-BCIP. Levels of pMdm2 and HDAC1 in each of

the sample were also estimated before precipitation following the standard protocol.

2.10. HDAC1 activity analysis

HDAC1 immunoprecipitates from nuclear fraction were eluted with 0.1 M glycine, pH 2.6 [34]. Extracted HDAC1 was incubated with pNA bound colorimetric substrate (Boc-Lys(Ac)-pNA) in absence or presence of trichostatin A on a shaker for 30 min at 37 °C. Reaction mixture was then incubated with lysine developer for 15-30 min and the produced chromophore can be analysed in an ELISA plate reader (Model 680, Microplate reader, Biorad Laboratory) at 405 nm.

2.11. HO1 activity assay

Isolated microsomal fractions were suspended in 100 mM potassium phosphate buffer (pH 7.4) containing 2 mM $MgCl_2$ before the initiation of HO1 assay. Activity of the enzyme was carried out by mixing 1 mg microsomal proteins, 2 mg cytosolic fraction (as the source of biliverdin reductase) to 100 mM potassium phosphate buffer (pH 7.4) containing 10 μM hemin, 2 mM Glucose-6-phosphate, 0.2 U of Glucose-6-phosphate dehydrogenase and 0.8 mM NADPH and incubated for 1 h at 37 °C in the dark. Reaction was terminated by the addition of 1 ml of chloroform. Amount of extracted bilirubin was calculated by measuring the difference in absorption between 464 and 530 nm (baseline absorbance) using an extinction coefficient of 40 mM^{-1} cm^{-1} for bilirubin [35].

2.12. PP2A phosphatase activity estimation

The protein phosphatase 2A activity of total cellular lysate was determined by malachite green-phosphate assay. Assay method is based on the formation of a complex between malachite green molybdate and free orthophosphate as described by the R&D Systems, Inc. In short, cell lysates were incubated in appropriate wells of microtiter plates coated with PP2A capture antibody and incubated on a rocking platform at 30 rpm for 3 h at 2-8° °C. After repeated washing, the serine/threonine phosphatase substrate was added so that the final concentration was 200 μM. Then the plate was incubated on a rocking platform at 30 rpm for 30 min at 37 °C. After incubation 10 μl of malachite green reagent A was added to each sample and incubated for another 10 min at room temperature. Lastly 10 μl of malachite green reagent B was added to each well and after 20 min of incubation colored product was estimated spectrophotometrically (UV-1240 Pharma Spec, Shimadzu) at 620 nm [36].

2.13. Measurement of mitochondrial membrane potential (MMP)

Mitochondrial membrane potential was evaluated by monitoring uptake and retention of the cationic carbocyanine dye JC1 into the mitochondrial matrix [37]. At first mitochondria was isolated from mice liver using mitochondria isolation kit (Sigma, St. Louis, MO, USA). Isolated mitochondria were incubated with 2 μl JC1 stain (from stock 1 mg/ml) and 950 μl JC1 assay buffer (20 mM MOPS, pH 7.5, containing 110 mM KCl, 10 mM ATP, 10 mM MgCl2, 10 mM sodium succinate, and 1 mM EGTA) for 10 min in dark at 25 °C. Percentage of green and red fluorescence positive cells was estimated flowcytometrically. Shifting of red to green fluorescence was measured spectrofluorimetrically and was represented in red to green fluorescence ratio.

2.14. Measurement of mitochondrial permeability transition (MPT)

MPT was measured by recording light scattering results from the swelling of mitochondria. The amount of light scattered is inversely proportional with the mitochondrial volume. MPT induction was monitored by incubating mitochondrial fraction (500 μg/ml) in respiration buffer pH 7.2 (125 mM sucrose, 50 mM KCl, 5 mM HEPES, 2 mM KH_2PO_4 and 1 mM $MgCl_2$). Alteration in the scattering of light due to swelling of mitochondria were estimated from the changes in absorbance at 540 nm over 15 min at room temperature in a UV–Vis spectrophotometer (UV-1240 Pharma Spec, Shimadzu) [38].

2.15. Cytochrome C quantification

The amount of cytochrome C present in mitochondrial and cytosolic fractions were analysed by using a commercially available cytochrome C ELISA kit (Rat/mouse cytochrome C Quantikine ELISA Kit, R&D Systems Inc. Minneapolis, USA) in accordance with the manufacturer's instructions [39]. After measuring the absorbance at 450 nm, cytochrome C concentrations were calculated by using the standard concentration curve. Values were represented in mitochondria to cytosolic ratio of cytochrome C.

2.16. Assessment of caspase3 activity

Caspase3 activity was determined spectrophotometrically (UV-1240 Pharma Spec, Shimadzu) using the immunosorbent caspase3 activity assay. In short, cell lysates were loaded in appropriate wells of microtiter plates coated with anti-active caspase3 antibody (caspase-3 p17 antibody) and incubated for 4 h at 4 °C. After washing, the substrate 100 μM Ac-DEVD-pNA was added. DEVD-dependent protease activity was determined by measuring the release of pNA spectrophotometrically at 405 nm [40].

2.17. Flow cytometric analysis for annexin V (AnV) binding

FACS analysis was performed to analyse the FITC labelled annexin V (FITC-AnV) binding to detect and quantify apoptosis and propidium iodide (PI) was to detect necrosis in the isolated hepatocytes by using a FACS Calibur (BD Biosciences, Mountain View, CA, USA) [41,42]. Hepatocytes were diluted 1:100 (5×10^7 hepatocytes/ml) by the binding buffer, pH 7.4 containing 10 mM HEPES–Na, 136 mM NaCl, 2.7 mM KCl, 2 mM MgCl2, 1 mM NaH_2PO_4, 5 mM glucose, 5 mg/ml BSA and 2.5 mM CaCl2. Annexin V-FTIC and PI were then added to a concentration of 1 μg/ml to each of the samples. Cell suspensions were then incubated for 15 min at room temperature in the dark. After incubation, an aliquot of the sample was taken out for flow-cytometric analysis. Percentage of apoptotic and necrotic cells were calculated using CellQuest software attached with the flow cytometer. FITC-positive and PI-negative cells were considered apoptotic, whereas PI-positive cells were considered necrotic and unstained cells were considered normal viable cells.

2.18. In situ assays for apoptosis

The terminal transferase dUTP end-labeling (TUNEL) assay was used to detect nicked or fragmented DNA in cryostat sections of liver. TUNEL assays were performed using [FITC] dUTP and terminal deoxynucleotide transferase. To detect nuclear conformation sections were further stained with propidium iodide (0.5 μg/mL) for 2 min at room temperature. The slides were rinsed thoroughly in PBS, cover-slipped and examined by fluorescence microscopy [43].

2.19. Histological study

Tissues from liver specimens were fixed overnight in 0.4 g/l phosphate-buffered paraformaldehyde. After fixation tissues were dehydrated and paraffin embedded according to the standard protocol. Sections about 5 μm thick were stained with hematoxylin and eosin for histological studies. Prepared slides were examined under light microscope (Model BX51 TRF, Olympus, Japan). Identified cells were counted and represented as number of cells/microscopic field.

2.20. Ki67 immunohistochemical analysis

Tissue sections were dewaxed in xylene and then were re-hydrated in alcohol. the endogenous peroxidase activity was blocked with 0.3% hydrogen peroxide and 0.1% sodium azide treatment for 15 min. Next sections were heated to 120 °C for 10 min in citrate buffer for antigen retrieval. Then they were rinsed in phosphate-buffered saline. Immunohistochemical staining for antibodies to Ki-67 were performed using the avidin–biotin–peroxidase complex method. At first primary antibody (1:1000) was applied to the sections and allowed to react for 1 h at room temperature. The sections were then incubated with biotinylated anti-mouse antibody (1:500 dilutions) for 25 min and avidin–biotin–peroxidase reagent for 25 min. After color development with diaminobenzimide, the sections were counterstained with hematoxylin [44].

2.21. Statistical analysis

Conventional method was used for the calculation of means and SEM. Statistically significant differences among treatment groups were evaluated by the Student's *t*-test. Data analysis was carried out using the GraphPad Instat software (Graph Pad, La Jolla, CA, USA). Differences were considered as statistically significant when $p < 0.05$.

3. Result

3.1. SAC in combination with berberine restored liver function more efficiently than individual drug treatment in the DEN + CCl4 exposed mice

Di-ethyl nitrosamine and carbon tetrachloride (DEN + CCl4) are potent environmental carcinogens. They can induce liver carcinogenesis in chronic exposure [20–22,45]. Here we treated the DEN + CCl4 exposed mice with SAC, an ingredient of aged garlic extract which is known to have antioxidant and hepatoprotective effects. Data showed that 250 mg/kg body weight SAC was able to decrease the aspartate transaminase (AST) (Fig. 1A) and alanine transaminase (ALT) (Fig. 1F) content while further increase in dose (upto 350 mg/kg body weight) did not exhibit significant additional reduction. Berberine, the candidate drug for cancer treatment with a hepatoprotective activity also had been included in the treatment schedule. Experimental analysis indicated that AST (Fig. 1B) and ALT (Fig. 1G) levels were reduced after berberine treatment at a dose of 8 mg/kg body weight. Although no such significant change was observed when the dose of the drug concentration was further increased to 12 mg/kg body weight. Now we were interested to assess the efficacy of the combination treatment of 8 mg/kg body weight berberine with 250 mg/kg body weight SAC against chronic DEN + CCl4 exposure. Result suggested significant reduction in both serum AST and ALT content in the individual SAC, berberine and most effectively in combined group after 30 days of treatment (Fig. 1C and H). Values were more and more ameliorated following another 30 days of post treatment (Fig. 1C and H) in the DEN + CCl4 exposed mice.

These effective concentrations of SAC, berberine and combined dose also showed their potency in maintaining the serum AST (Fig. 1D) and ALT (Fig. 1I) to normal range in the co-treated groups (individual SAC or berberine or in combined treatment) of DEN + CCL4 exposed mice.

Effectiveness of the selected dose was again confirmed by the lactate dehydrogenase (LDH) and alkaline phosphatase (ALKP) assay. Data demonstrated efficient diminution of LDH and ALKP in SAC-, berberine- and combined post treated group (Fig. 2A and D). The dose also retained serum LDH (Fig. 2B) and ALKP (Fig. 2E) activities towards normal after 90 days of co-treatment (individual SAC or berberine or in combined treatment) in carcinogen exposed group.

Moreover, serum AST (Fig. 1E), ALT (Fig. 1J), LDH (Fig. 2C), ALKP (Fig. 2F) assay indicated that administration of selected dose of SAC and berberine alone or in combination did not exert any toxicity to the control mice after 60 days of treatment.

3.2. Effect of drug treatment on the DEN + CCl4 induced hepatic morphological alterations in mice

Macroscopically, gray-white nodular patches were identified from the surrounding reddish brown background surface of liver in DEN + CCl4 exposed mice (Fig. 3B). Some of the gray-white nodular patches were still seen in the individual treatment of SAC (Fig. 3F) and berberine (Fig. 3G) while surface of the liver had a nailed appearance due to presence of hypo-intense light brown spots in combined group (Fig. 3H) after 30 days of post treatment. Continuation of the treatment for another 30 days (Fig. 3I) illustrated complete disappearance of all white or light brown spots and morphologically look alike with that of control. Co-treatments (individual SAC or berberine or in combined treatment) with the selected dose (Fig. 3C, D and E) maintained normal morphological pattern of the liver. Data was most satisfactory (Fig. 3E) in the combined group.

3.3. SAC and berberine treatment reduced cell proliferation and diminished CYP2E1 mediated oxidative stress in liver of DEN + CCl4 exposed mice

CyclinD1 is a nuclear protein required for cell cycle progression in G1. The overexpression of this protein has been linked to the development and progression of hepatocellular carcinoma [46]. Report suggested the involvement of cyclinD1 in the DEN induced progressive liver carcinogenesis [47]. In accordance with the information our experimental analysis also displayed increased expression of cyclinD1 (Fig. 4A) in the DEN + CCl4 exposed mice. While SAC and berberine individually and more efficiently in combination (19.13% against SAC; $p < 0.02$ and 27.059% against berberine; $p < 0.01$) reduced cyclinD1 expression in the post treated group. Another 30 days treatment with a break of 10 days represented more or less similar expression of cyclinD1 with respect to control animal (Fig. 4B).

Proliferating cell nuclear antigen (PCNA) expression and synthesis are closely linked with cell proliferation. Being a cell proliferation marker it plays an important role in the development of nodules during the progress of hepatocarcinoma [45]. Data demonstrated distinct high concentration of PCNA (Fig. 4A) as expressed by the densitometric analysis (Fig. 4C) in the DEN + CCl4 exposed mice. Expression was significantly reduced after SAC and berberine post treatment and more efficiently in the combined (SAC + berberine) group (22.22%, $p < 0.02$ against SAC and 32.039%, $p < 0.01$ against berberine) group. Treatment continuation with combined drug for an additional 30 days with a break of 10 days exhibited more or less similar concentration of PCNA as comparable to the control mice.

Co-treatment with SAC-, berberine- and combined drug (SAC + berberine) did not show any significant change in PCNA and cyclinD1 (Fig. 4A, B and C) expression with respect to control mice. Although combined group was more competent in the reduction of PCNA and cyclinD1 than either SAC or berberine individual treatment.

Ki67 is another useful marker of cell proliferation. Immunoreactivity of the protein is localized in nucleus mainly in the nucleolus and nuclear membrane. The numbers of Ki67 positive cells were increased significantly in carcinogen exposed group (Fig. 4E). 30 days of post treatment with SAC, berberine and more effectively the combined group limited Ki67 expression in the DEN + CCl4 exposed mice. Additional treatment with the combined drug for another 30 days reduced the number of Ki67 positive cells and the result was similar to control.

In the co-treated group SAC and berberine maintained reduced Ki67 expression. Combined group exhibited insignificant number of Ki67 positive cells in the immunohistochemical analysis.

Cell proliferation markers have a potential prognostic significance towards development of hepatocarcinoma [48], which is dependent upon bioactivation of hepatocarcinogen. It is reported that cytochromeP4502E1 (CYP2E1) mediated alkylation is responsible for the metabolic activation of DEN [49]. The enzyme is also involved in the stimulation of CCl4 induced hepatocarcinogenesis through reductive dehalogenation

[50]. Our data indicated reduction in the expression of CYP2E1 after SAC-, berberine- and most significantly in the combined drug treated group of co-treated as well as of the post treated (30 days) DEN + CCl4 exposed mice (Fig. 4A). In the co treatment combined group showed 32.39% reduction ($p < 0.01$) in the densitometric value from SAC and 40% reduction ($p < 0.01$) from berberine treated group. While study

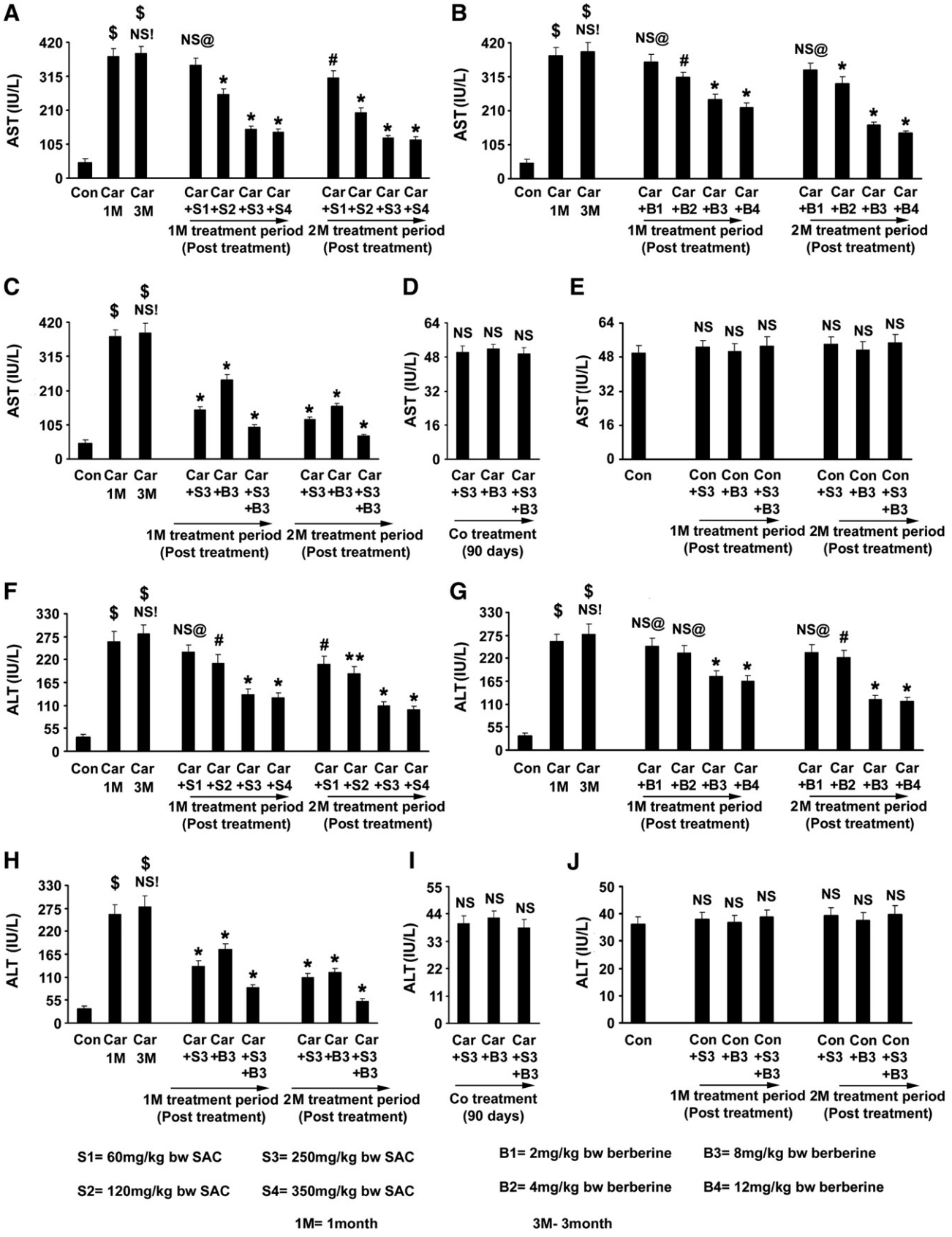

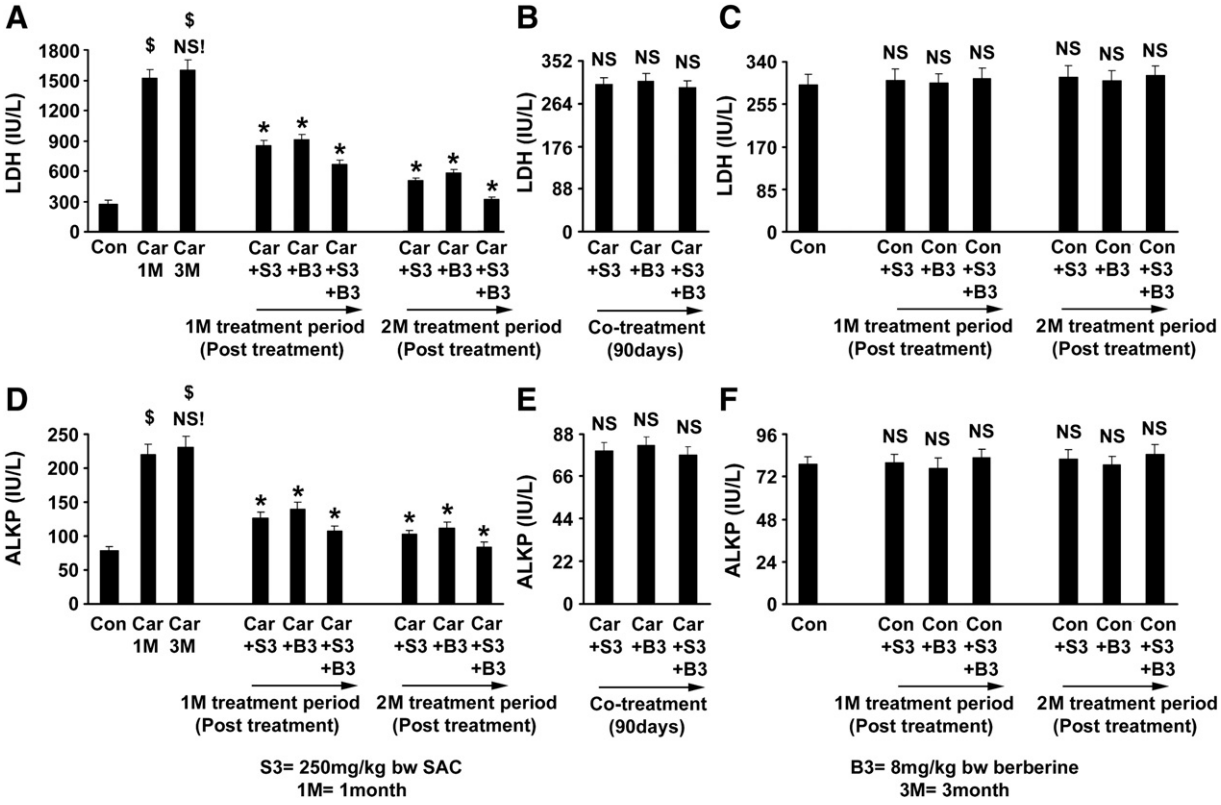

Fig. 2. Determination of LDH and ALKP activities after SAC and berberine treatment. (A) LDH activity and (D) ALKP activity were evaluated in DEN + CCl4 exposed mice following SAC (250 mg/kg body weight) and berberine (8 mg/kg body weight) or in combined post treatment. After 30 and 60 days (with drug) plus 10 days (without any drug) the enzymatic activities were assessed. Values are mean ± SD of five independent experiments (n = 4). $p < 0.01 vs control mice. NS! against 1 month carcinogen exposed group and *p < 0.01 vs. 3 month carcinogen exposed group. Regulation of LDH activity (B) and ALKP activity (E) in co-treatment with 250 mg/kg body weight SAC, 8 mg/kg body weight berberine and in combined group were analyzed. Serum LDH and ALKP activities in drug treated control animal (in single or in combination with 250 mg/kg body weight SAC and 8 mg/kg body weight berberine) were monitored for toxicity analysis. Data are mean ± SD of five independent experiments (n = 4). NS vs. control group.

on the post treated group presented 34% reduced expression ($p < 0.01$) of CYP2E1 from SAC and 47.62% reduction ($p < 0.01$) from berberine treated group. Though after another 30 days of combined drug treatment followed by 10 days of without any drug treatment demonstrated the regaining of enzyme expression (Fig. 4A and D).

Activity assay of the CYP2E1 (Fig. 4F) indicated higher value in the DEN + CCl4 exposed mice although enzyme expression remained more or less same to the control ones. Enzyme activity was effectively decreased after combined treatment for 30 days and further progression of the treatment of another 30 days reduced the value towards control level. Co-treatment indicated insignificant change in the enzyme activity. Our next attempt was to evaluate the CYP2E1 induced oxidative stress in the DEN + CCl4 exposed mice (Fig. 4G). To this end, we found that percentage of DCFDA fluorescence positive cells (67.9%) were decreased in SAC- (35.7%), berberine- (41.83%) and significantly after 30 days of combined treatment (23.13%) in the post treated group. Experimental analysis indicated effective diminution of TBARS (Fig. 4H), a potential marker of oxidative stress after 30 days of combined treatment of SAC and berberine in comparison to their individual treatment. While additional treatment of SAC + berberine for another 30 days reduced the value of the DCFDA positive cells to only 8.98% (Fig. 4G) and the TBARS value was reverted back towards control (Fig. 4H).

In the co-treatment, SAC (11.9% DCFDA positive cells) and berberine (19.11% DCFDA positive cells) individually prevent accumulation of ROS to some extent. Significant shifting of histogram towards left indicated provision of effective inhibition of DCFDA fluorescence (6.9% DCFDA positive cells) in SAC + berberine treated group (Fig. 4G). Data was further reflected in the TBARS analysis where protection of membrane lipids from oxidation were revealed after SAC-, berberine- and specifically the combined treatment of DEN + CCl4 exposed mice (Fig. 4H).

3.4. Regulation of antioxidant status in liver of DEN + CCl4 exposed mice with SAC and berberine treatment

Reduction of oxidative stress after drug treatment instructed us to determine the status of hepatic antioxidant potential in treated groups of DEN + CCl4 exposed mice. Taking into account the potential reducing capacity of the reduced glutathione (GSH) at first the redox potential of the glutathione system in liver was estimated. Fig. 5A showed

Fig. 1. Estimation of serum AST and ALT activities in swiss albino mice. Post treatment with SAC (60, 120, 250, 350 mg/kg body weight) and berberine (2, 4, 8, 12 mg/kg body weight) was started after 90 days of DEN + CCl4 exposure and continued for the 60 days. Carcinogen (DEN + CCl4) exposed mice were sacrificed after 90 days of exposure. In the co-treated group animals were treated with SAC (250 mg/kg body weight) and berberine (8 mg/kg body weight) from the first day of carcinogen exposure upto 90 days. Details of treatment schedule are given in the Materials and methods section. Effect of various doses of SAC and berberine on AST (A and B) and ALT (F and G) activities were represented. In the post treated groups mice were sacrificed after 30 and after 60 days with a gap of 10 days for experimental analysis. Consequences of SAC and berberine combination treatment on the AST (C) and ALT (H) activities in the serum with the progress of treatment. Results are mean ± SD of five independent experiments (n = 4). $p < 0.01 vs control mice. NS! against 1 month carcinogen exposed group. NS@, #p < 0.05, **p < 0.02 and *p < 0.01 vs. 3 month carcinogen exposed group. (D) and (I) demonstrated the result of SAC and berberine or combined co-treatment on AST and ALT activity, respectively. Control animals were treated with 250 mg/kg body weight SAC and 8 mg/kg body weight berberine as well as in combination for 60 days. AST (E) and ALT (J) activities were analyzed for toxicity assay. Values are mean ± SD of five independent experiments (n = 4). NS vs. control group.

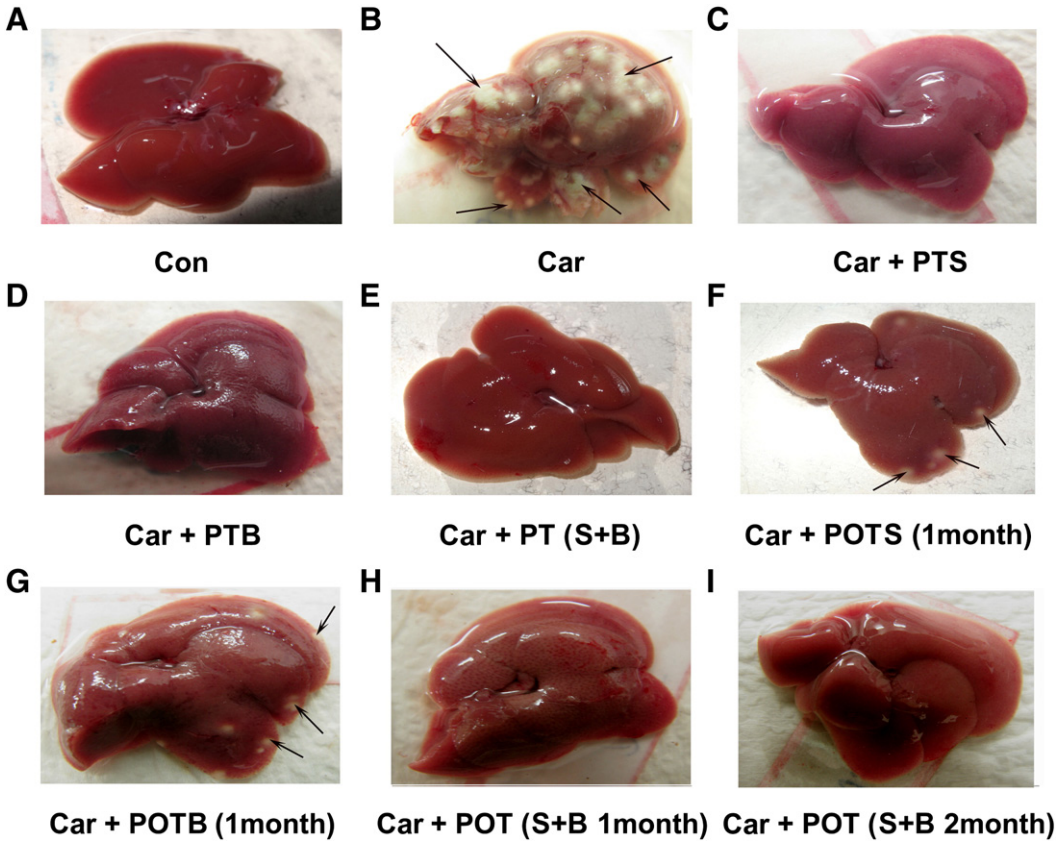

Fig. 3. SAC + berberine ameliorated hepatocarcinoma. Hepatic morphological structure corresponded to (A) control; (B) 90 days DEN + CCl4 exposed mice; co-treated with (C) SAC, (D) berberine and (E) SAC + berberine for 90 days; post treatment after 90 days of carcinogen exposure with (F) SAC, (G) berberine and (H) SAC + berberine for 30 days; as well as combined treatment of SAC + berberine for another 30 days with a gap of 10 days (I). Arrows indicate hepatocarcinogenic nodules. Representative results from six independent animals from each group are exhibited. PT = Co-treated; POT = Posttreated; S = SAC treated; B = berberine treated and S + B = SAC + berberine treated group.

level of reduced glutathione was greatly impaired in the DEN + CCl4 exposed mice. Individual treatment with berberine demonstrated insignificant change in the GSH content in comparison to carcinogen exposed group. However increase in GSH content appeared to be significant in SAC- and specifically in combined group. Continuation of the experimental study with combined drug almost fully rectified GSH content during the course of another 30 days treatment. In the co-treated groups, drugs efficiently retained GSH content and the value of SAC + berberine treated set was approximately same as to the control. Next we want to investigate the effect of SAC and berberine administration on the antioxidant enzymes involved in the detoxication of ROS. For this study isolated mitochondrial and cytosolic fractions were blotted against β actin and VDAC1/porin antibody respectively (Fig. 5B). Absence of β actin in mitochondrial extract and VDAC1/porin in the cytosolic extract indicated successful separation of mitochondrial fraction from cytosolic fraction of liver cells. Activity assay followed by zymographic analysis of Cu-Zn SOD in the cytosolic compartment (Fig. 5E and F) and Mn SOD within mitochondria (Fig. 5C and D) were in good agreement with the redox status of glutathione before and after the treatment and also in co treated group. Enzymatic activities were most efficiently regained after the combined SAC and berberine treatment. Beside this we noticed the reduction of catalase activity by examining enzymatic assay (Fig. 5H) and zymographic analysis (Fig. 5G) following DEN + CCl4 exposure. Antioxidant capacity of the said enzyme was retrieved in SAC-, berberine- and successfully after combined drug treatment. Therapeutic extension of the combined post treatment for another 30 days almost repaired Cu-Zn SOD, Mn-SOD and catalase activities. In the co-treatment, trivial reduction in catalase activity with respect to control was observed in the berberine treated group. While treatment with SAC- and specially combined drugs showed their ability in the maintenance of the activities of enzymatic antioxidants.

3.5. Treatment with SAC and berberine modulated hepatic Nrf2/HO1 activity in DEN + CCl4 exposed mice

Oxidative stress activates Nrf2 which is important for protecting cells against oxidative damage [51]. Capacity of cells to sustain homeostasis during oxidative stress is maintained by the activation of protective enzymes. Transcriptional activation of those protective antioxidant genes through an antioxidant response element (ARE) is largely dependent upon the function of Nrf2 [51] as transcription factor. Thus we wanted to examine the effect of generated oxidative stress on Nrf2 expression in the carcinogen exposed group. For the experimental purpose we first isolated nuclear fraction from cytosolic fraction. Further the nuclear extracts and cytosolic extracts were blotted against β actin and lamin B antibody respectively (Fig. 6A and B). Absence of β actin in nucleus and lamin B in cytosolic extract suggested the successful separation of nuclear fraction from cytosolic fraction. Fig. 6A and B indicated significant higher expression of Nrf2 both in cytosolic (2.28 fold against control) and in nuclear fraction (3.3 fold against control) of hepatocytes isolated from DEN + CCl4 exposed group. Moreover, increased expression of protein was sustained as suggested by the immuno blot analysis (inset of Fig. 6A and B) after 30 days of post treatment. Berberine-, SAC- and combined drug treated group represented 1.61, 1.81 and 1.92 fold higher Nrf2 expression in cytoplasmic portion as well as 2.03, 2.29 and 2.43 fold increased Nrf2 expression in nuclear portion respectively against control (Fig. 6A and B).

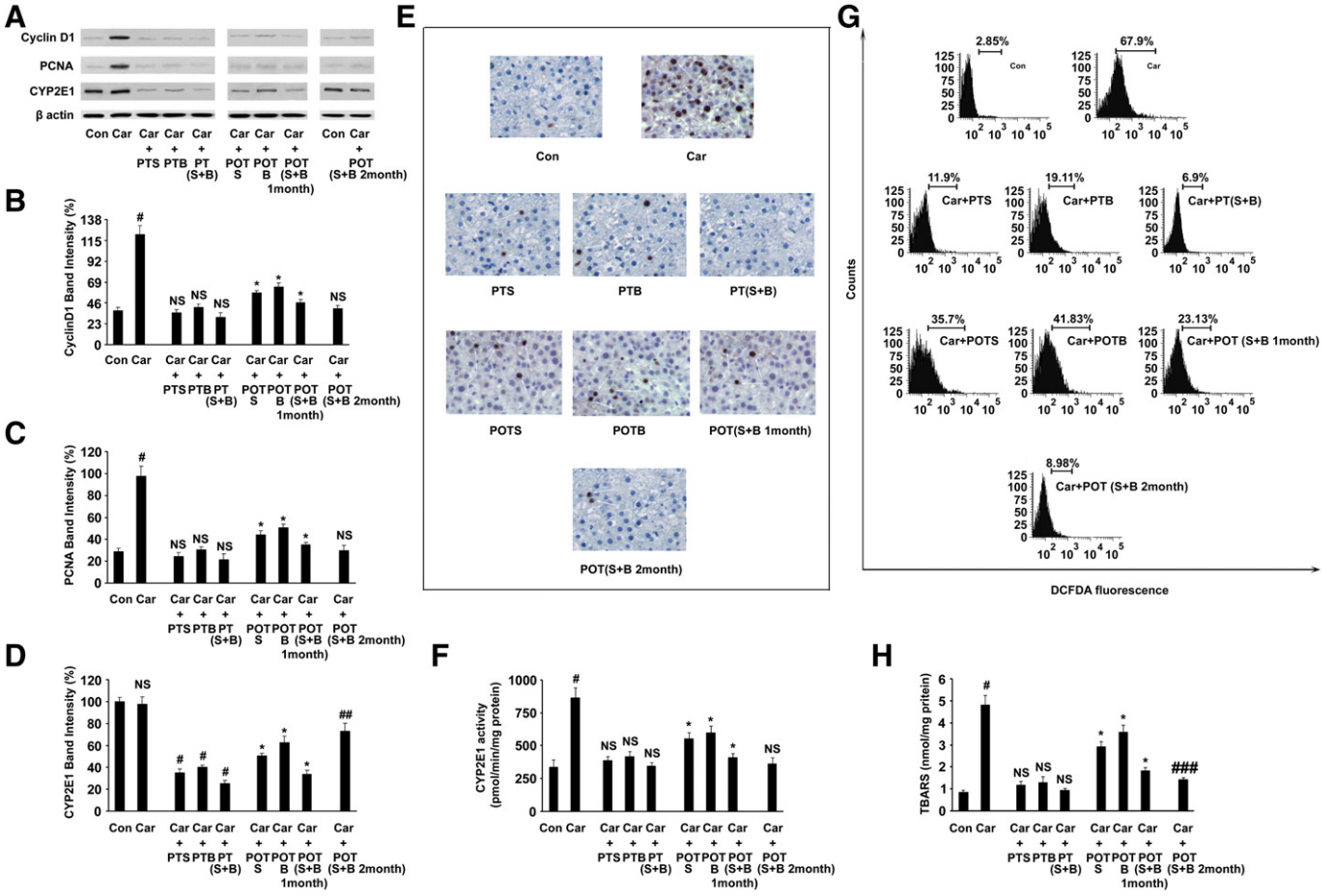

Fig. 4. SAC and berberine control CyclinD1, PCNA, CYP2E1 expression and oxidative stress in hepatocytes of DEN + CCl4 exposed mice. (A) Immuno blot analysis of cyclinD1, PCNA and CYP2E1 in the hepatocytes isolated from control, carcinogen exposed, SAC and berberine treated groups. An identical blot of β-actin served as loading control. Densitometric analysis of cyclinD1 (B), PCNA (C) and CYP2E1 (D) immunoblots in control, carcinogen and drug treated groups were represented. (E) Ki67 expression within control, carcinogen and drug treated group were analyzed immunohistochemically following avidin-biotin-peroxidase complex method. Tissue sections were counterstained with hematoxylin as described under the Materials and methods section. (F) CYP2E1 activity analysis in the hepatocytes of control, carcinogen exposed and SAC, berberine treated mice. Isolated liver microsomal protein was incubated with para-nitro-phenol containing assay mixture at 37 °C for 30 min. After TCA precipitation generation of para-nitro-catechol was assessed spectrophotometrically. Results are mean ± SD of five independent experiments (n = 4). NS, ##$p < 0.02$ and #$p < 0.01$ vs. age matched control group; *$p < 0.01$ vs. carcinogen group.(G) FACS analysis after binding of hepatocytes (1×10^5) to DCFDA for determining the ROS generation within hepatocytes of control, carcinogen and SAC, berberine treated mice as described under Materials and method section. Results are representative of four independent experiments. (H) Oxidative stress on membrane lipids of hepatocytes were analysed by measuring TBARS production in control, carcinogen and drug treated group. Results are the mean ± SD of five independent experiments (n = 4). NS, ###$p < 0.05$ and #$p < 0.01$ vs. age matched control group; *$p < 0.01$ vs. carcinogen group. PT = Co-treated; POT = Post-treated; S = SAC treated; B = berberine treated and S + B = SAC + berberine treated group.

Since hemoxygenase-1(HO-1) is the downstream anti-oxidative stress enzyme of Nrf2, we next examined protein expression of the said enzyme after drug treatment in the DEN + CCl4 exposed mice. Fig. 6C depicted the increased expression of HO1 (1.9 fold against control) in the carcinogen exposed group probably to combat oxidative stress. In the post treated group expression of this enzyme remained higher after 30 days of berberine- (1.31 fold against control), SAC- (1.39 fold against control) and combined drug (1.46 fold against control) treatment. Change in HO1 expression in the combined group was insignificant with respect to SAC treatment while 9.736% increased expression ($p < 0.05$) was observed against berberine individual treatment. Therefore change in the HO1 expression in the combined post treated group was more or less comparable to SAC and an increased value was observed against berberine individual treatment. Result suggested that berberine did not show any additional effect on HO1 expression as compared with the treatment with S-allyl cysteine in the combined group of mice.

Further continuation of another 30 days combined drug treatment and a subsequent exclusion of any drug for 10 days indicated regaining of the status of Nrf2 and HO1 more or less similar to the control (1.02 fold change in nuclear fraction and 1.06 fold change in cytosolic fraction of Nrf2 as well as 1.11 fold change of HO1 considering the expression of control mice) as demonstrated by Fig. 6A, B and C. During co-treatment also there were significant increase both in the Nrf2 and HO1 expression in all the treated groups (Fig. 6A, B and C).

Assay of the HO1 indicated keeping up of enzymatic activity after 30 days of post treatment with berberine and SAC individual treatment. Combination of SAC and berberine maintained HO1 activity 13.66% high against SAC ($p < 0.05$) and 40.31% high against berberine ($p < 0.01$) individual treatment (Fig. 6D). Activity was diminished in the mice of post treated group after additional treatment with combined drugs for 30 days and a subsequent break in the drug treatment for 10 days. Study indicated that co-treatment with SAC-, berberine- and in combination showed valuable increase in the HO1 activity with respect to control level which was in agreement with the result presented in Fig. 6CD.

Result indicated the involvement of SAC and berberine in somehow retaining of Nrf2/HO1 activity during treatment period. Inhibition of generation of oxidative stress in the co-treated groups (Fig. 4G) together with the reduced activity of Nrf2/HO1 pathway (Fig. 6) in comparison to the post treated groups after 30 days of treatment defined the role of ROS accumulation in SAC and berberine mediated maintenance of Nrf2/HO1 pathway.

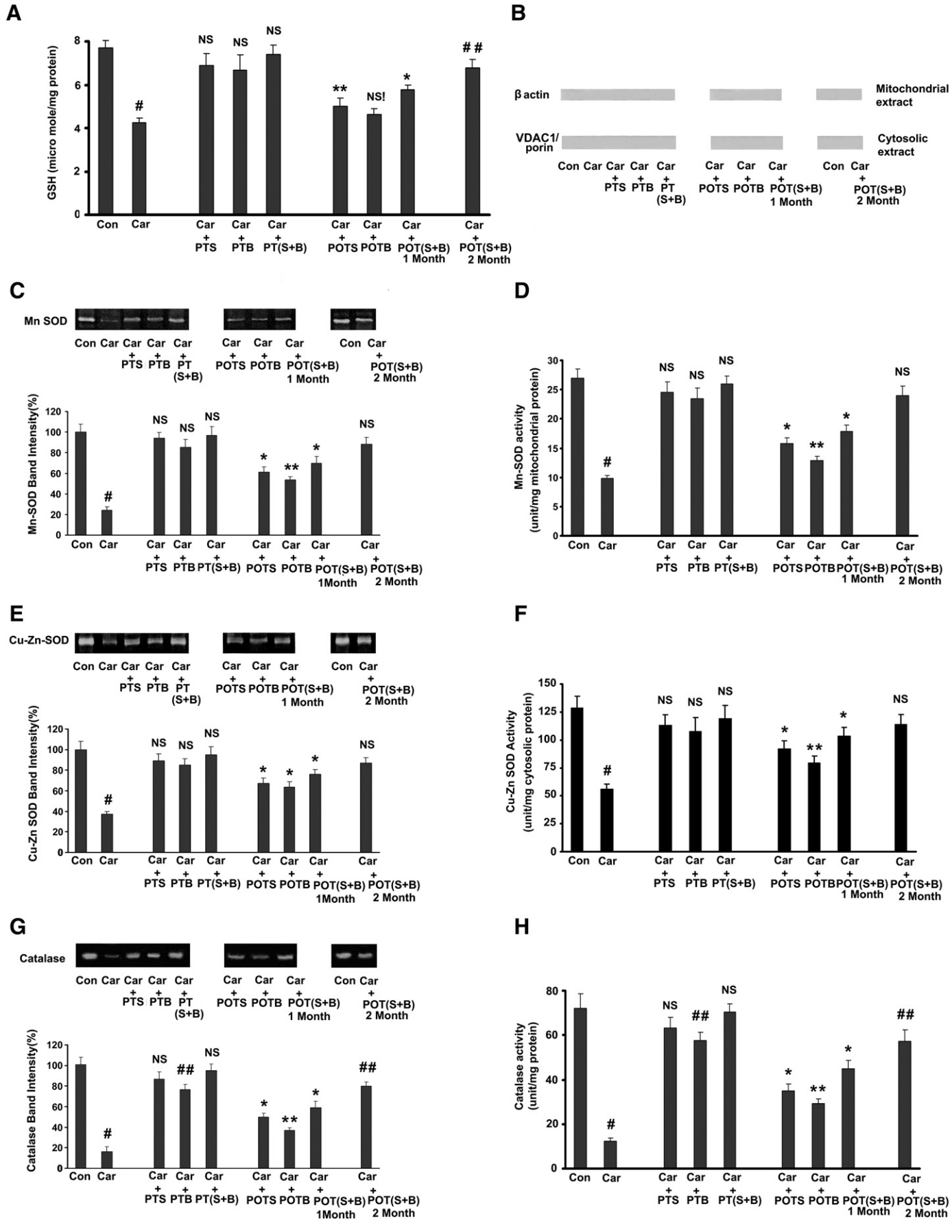
A
GSH (micro mole/mg protein)
Con Car Car + PTS Car + PTB Car + PT(S+B) Car + POTS Car + POTB Car + POT(S+B) 1 Month Car + POT(S+B) 2 Month
B
β actin
VDAC1/ porin
Mitochondrial extract
Cytosolic extract
C
Mn SOD
Mn-SOD Band Intensity(%)
D
Mn-SOD activity (unit/mg mitochondrial protein)
E
Cu-Zn-SOD
Cu-Zn SOD Band Intensity(%)
F
Cu-Zn SOD Activity (unit/mg cytosolic protein)
G
Catalase
Catalase Band Intensity(%)
H
Catalase activity (unit/mg protein)

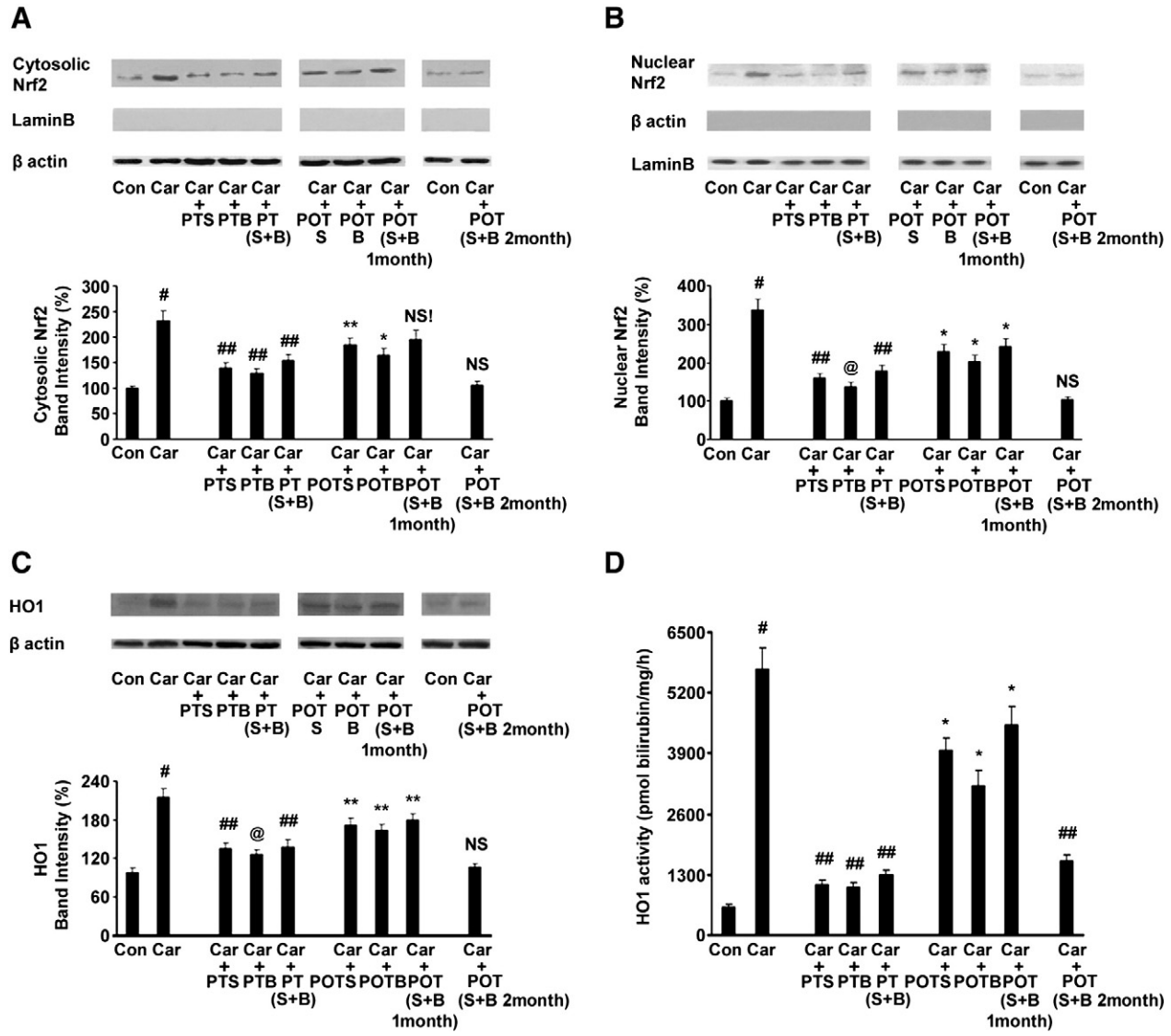

Fig. 6. Treatment with SAC and berberine modifies Nrf2-HO1 pathway within hepatocytes of DEN + CCl4 exposed mice. Cell lysates were fractionated into cytosolic and nuclear portion. Each of the fractions was separated by SDS-PAGE and immunoblotted using anti-Nrf2 antibody. Analysis of cytosolic Nrf2 (A; upper panel) and nuclear Nrf2 (B; upper panel) were performed with the respective fractions isolated from hepatocytes of control, carcinogen exposed and SAC, berberine treated group. HO1 analysis was conducted in the microsomal fraction and the protein was immunoblotted using anti-HO1 antibody after SDS-PAGE separation in control, carcinogen exposed and drug treated group (C). An identical blot of β-actin served as loading control. Densitometric analysis of immunoreactive bands is represented in the lower panel of (A), (B) and (C). (D) For enzymatic analysis of HO1 microsomal fraction was incubated with biliverdin reductase, hemin and NADPH at 37 °C for 1 h. Change in the amount of extracted bilirubin was determined spectrophotometrically in the control, carcinogen exposed and drug treated group. Results are the mean ± SD of five independent experiments (n = 4). @$p < 0.05$, ##$p < 0.02$ and #$p < 0.01$ vs. age matched control group; NS!, *$p < 0.01$ and **$p < 0.05$ vs. carcinogen group. PT = Co-treated; POT = Post-treated; S = SAC treated; B = berberine treated and S + B = SAC + berberine treated group.

3.6. Regulation of proapoptotic-antiapoptotic status in liver of DEN + CCl4 exposed mice with SAC and berberine treatment

Since knock down of HO1 already proved its relevance in the modification of Bcl-2/Bax ratio [52], we next examined the effect of increased HO1 expression on antiapoptotic protein Bcl2 in DEN + CCl4 exposed mice. Fig. 7A indicated significant increase of Bcl2 expression in carcinogen exposed group, which was decreased only moderately in SAC-, berberine- and combined group after 30 days of post treatment possibly due to retaining of the HO1 expression to some extent and specifically the enzymatic activity in the post treated group. When the combined treatment was carried on for further 30 days and after that a gap for 10 days showed more or less reversal of the expression towards control level. Co-treatments with berberine- and also in SAC- and combined

Fig. 5. Effect of SAC and berberine treatment on the anti-oxidant system present in hepatocytes of DEN + CCl4 exposed mice. (A) Reduced glutathione level of hepatocytes was estimated as described in Materials and method section. Results are the mean ± SD of five independent experiments (n = 4). NS, ##$p < 0.05$ and #$p < 0.01$ vs. age matched control group; NS!, *$p < 0.01$ and **$p < 0.05$ vs. carcinogen group. (B) β actin and VDAC1/porin content were estimated in mitochondrial extract and cytosolic extract respectively. Cytosolic Cu-Zn SOD (E; upper panel) and (C; upper panel) mitochondrial Mn-SOD zymography were performed by running the cytosolic as well as mitochondrial fraction of hepatocytes in non-reducing SDS-PAGE followed by staining with TEMED and riboflavin. Enzymatic activity of Cu-Zn SOD (F) and Mn-SOD (D) were further assayed by measuring 50% inhibition of $O_2^{\bullet -}$-mediated oxidation of pyrogallol as demonstrated in the Materials and methods section. Catalase zymography (G; upper panel) were developed by incubating the non-reducing SDS-PAGE of cell extract with horseradish peroxidase and then with H_2O_2 to identify the activity of enzyme. Densitometric analysis of zymograms (lower panel of E, C and G) of control, carcinogen exposed and drug treated animals were represented. Spectrophotometrically catalase activity (H) was assessed in the respective groups by measuring the breakdown of H_2O_2. Values are the mean ± SD of five independent experiments (n = 4). NS, ##$p < 0.05$ and #$p < 0.01$ vs. age matched control group; *$p < 0.01$ and **$p < 0.02$ vs. carcinogen group. PT = Co-treated; POT = Posttreated; S = SAC treated; B = berberine treated and S + B = SAC + berberine treated group.

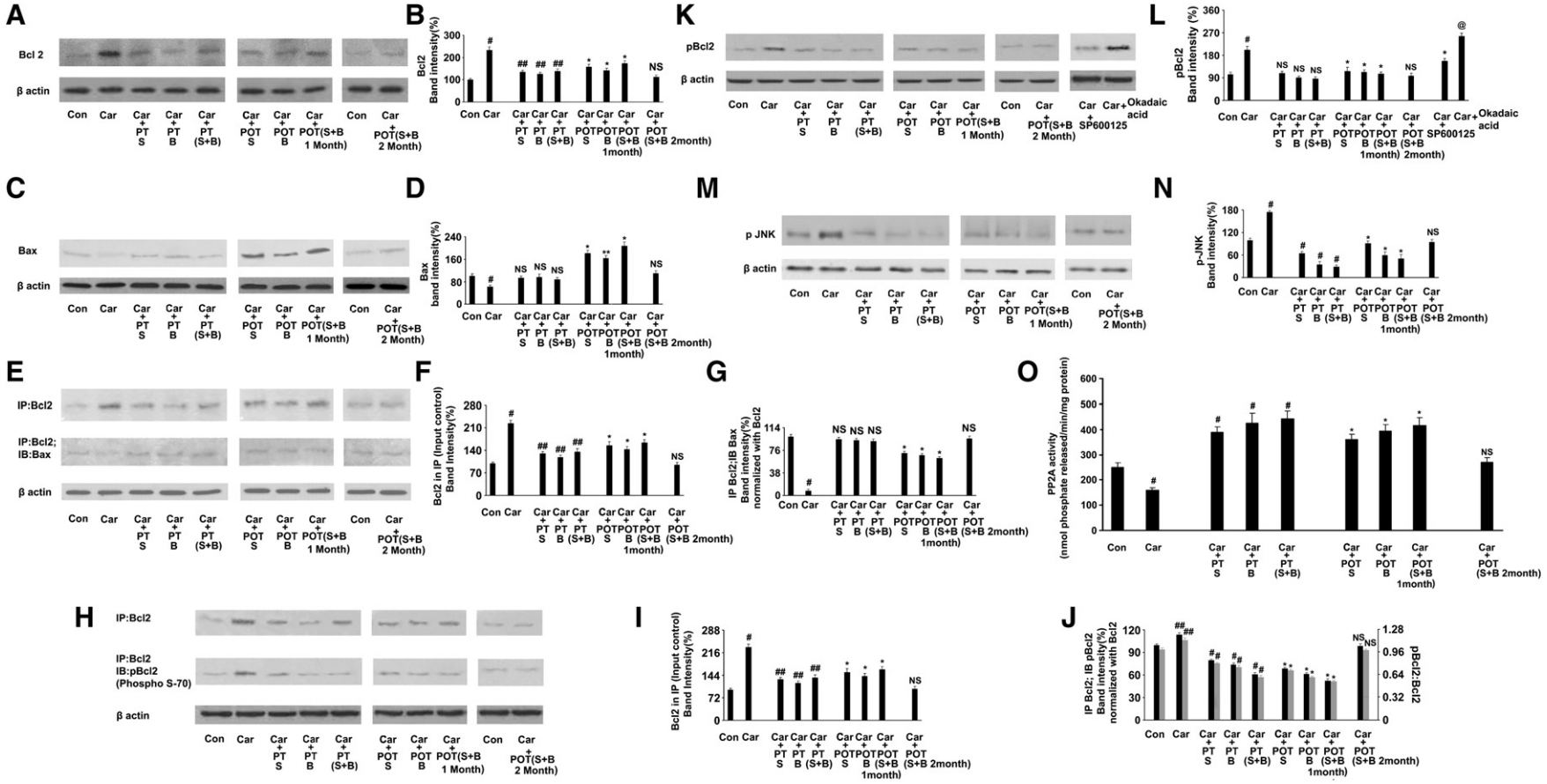

Fig. 7. Consequences of SAC and berberine treatment on the proapoptotic-antiapoptotic homeostasis present within hepatocytes of DEN + CCl4 exposed mice. Hepatocytes isolated from control, carcinogen exposed, SAC, berberine, pJNK inhibitor (SP600125) and PP2A inhibitor (okadaic acid) treated group were lysed in RIPA buffer. Cell lysates were separated by SDS-PAGE and protein expressions were assessed by using respective antibodies; such as (A) anti-Bcl2, (C) anti-Bax, (K) anti-pBcl2 and (M) anti-pJNK. Blot with anti-β-actin served as loading control. (E) Aliquots of cell lysates of control, carcinogen exposed and SAC, berberine treated groups were subjected to immunoprecipitation using antibody against Bcl-2 followed by immunoblotting using anti-Bax antibody. Level of immunoprecipitated Bcl2 was also determined before immunoblotting with anti-Bax antibody. (H) Bcl2 phosphorylation was evaluated by immunoprecipitating Bcl2 from cell lysate and subsequent immuno blot analysis against anti-Phospho-Bcl-2 [pSer70]. Bcl2 level was also estimated by blotting the sample with anti-Bcl2 before and after precipitation. Densitometric analysis of respective immunoblots of Bcl2 (B), of Bax (D), of IP: Bcl2 and IB: Bax, values were normalized against Bcl2 (G), of IP Bcl2 (input control) (F), of IP: Bcl-2 and IB: pBcl2, values were normalized against Bcl2 (J), of IP Bcl2 (input control) (I), of pBcl2 (L) and of pJNK (N) were represented. (O) PP2A activity in the cell lysate of control, carcinogen exposed and drug treated group was measured using immunoprecipitation phosphatase assay kit from R&D System as described in the Materials and methods section. Results are expressed in terms of liberated phosphate concentration which was measured spectrophotometrically after addition of malachite green phosphate detection solution. Values are the mean ± SD of five independent experiments (n = 4). NS, ##p < 0.05 and #p < 0.01 vs. age matched control group; @p < 0.02, *p < 0.01 and **p < 0.05 vs. carcinogen group. PT = Co-treated; POT = Post-treated; S = SAC treated; B = berberine treated and S + B = SAC + berberine treated group.

group Bcl2 band intensity remained high than the control value as demonstrated by the densitometric analysis (Fig. 7B). It is possibly due to increase in HO1 expression as well as activity in co-treated groups of DEN + CCl4 exposed mice (Fig. 6C and D). Investigation of the proapoptotic protein Bax indicated considerable reduction of the protein in the DEN + CCl4 exposed group (Fig. 7C). During co-treatment the expression of the Bax more or less same after berberine treatment and is somehow reduced after SAC as well as in combined treatment (Fig. 7C). Although according to the densitometric analysis (Fig. 7D) changes were not significant in comparison to control. While data showed significant induction of Bax in the post treated groups after 30 days of treatment. Continuation of the treatment brought back the protein concentration towards near about control (Fig. 7C and D).

Co-immunoprecipitation (Co-IP) of Bax with Bcl2 (Fig. 7E) displayed the status of Bcl2-Bax interaction, which determined fate of the hepatocytes. Fig. 7A and C represented the relative level of Bcl2 and Bax before precipitation. Fig. 7E and F demonstrated Bcl2 immunoprecipitation. Densitometric analysis of Bax co-immunoprecipitation was evaluated after normalization with Bcl2 (Fig. 7G). Data revealed a trivial presence of Bax protein in the coimmunoprecipitates of carcinogen exposed group. There was insignificant change in Bax concentration in the anti Bcl2 immunoprecipitates of co-treated groups with respect to control as observed in Fig. 7G. Band intensities of co-IP Bax were significantly increased in post treated groups with respect to carcinogen exposure. Moreover, post treatment represented 11.72% decreased co-immunoprecipitation of Bax with Bcl2 (Bcl2-Bax interaction) ($p < 0.05$) in the combined group against SAC and only 4.75% reduction (insignificant change) was observed with respect to berberine individual treatment. Co-treatment exhibited minor change (3.46% decrease, insignificant) in Bax coimmunoprecipitation with Bcl2 (Bcl2-Bax interaction) in the combined co-treated group with respect to SAC and an insignificant change (only 1.66%) against berberine individual treatment. Densitometric analysis also demonstrated decreased co-immunoprecipitation of Bax in the post treated groups (28.25% decrease in SAC, 33.5% decrease in berberine and 36.66% in combined post treatment with respect to control after normalization with Bcl2; $p < 0.01$) indicating drop in Bcl2-Bax interaction in comparison with control group. Continuation of the combined treatment did not show any observable difference with respect to control mice (Fig. 7G).

To better understand the ambiguities regarding the reduction of Bcl2-Bax interaction in the presence of high concentration of Bax and reasonable higher concentration of Bcl2 in the 30 days of post treated group with respect to control, we analyzed the status of Ser70 phosphorylation of Bcl2 because it is the prerequisite for Bcl2-Bax interaction [53]. Level of precipitated Bcl2 was demonstrated in Fig. 7H and was densitometrically analyzed in Fig. 7I. Data suggested significant increase of Bcl2 immuno-precipitation in carcinogen exposed group and an effective reduction was observed following SAC-, berberine individual and specifically after 30 days of combined post treatment. The effect was possibly due to modification of Bcl2 expression in the DEN + CCl4 exposed and drug treated groups as observed in Fig. 7A. Another 30 days treatment with combined drug exhibited insignificant change with respect to control. Co treatment with the drugs also displayed almost similar trend as depicted in Fig. 7A. Fig. 7H demonstrated level of phosphorylated Bcl2 and data was densitometrically analyzed in Fig. 7J after normalizing with total Bcl2. Ratio of phosphorylated Bcl2 over total Bcl2 was also estimated and was represented in Fig. 7J. Result showed reduction in Bcl2 phosphorylation in co-treatment and after 30 days drug treatment specifically in berberine and combined post treated group. 26.517% ($p < 0.01$) diminution in pSer70Bcl2 level in SAC + berberine treated group with respect to SAC treatment and 19.18% ($p < 0.02$) reduction against berberine treated group was observed in the post treated group. Co-treatment demonstrated 22.67% ($p < 0.01$) decrease and 16.6% ($p < 0.02$) fall in pSer70Bcl2 level in the combined drug treated group with respect to SAC and berberine individual treatment, respectively. 60 days of post treatment (Fig. 7H and J) did not show any impressive change in Bcl2 phosphorylation with respect to control.

Fig. 7K represented total pBcl2 level and percentage of band intensity was displayed in Fig. 7L. Result suggested increased phosphorylation of Bcl2 in the carcinogen exposed group. Post treatment with the SAC-, berberine and combined drugs displayed trivial increased level of pBcl2 with respect to control and value was substantially decreased from the DEN + CCl4 exposed group. In the co treated group changes in pBcl2 level were insignificant against control. Level of Bcl2 phosphorylation was somehow reduced in the berberine treated and combined group. 30 days extension of combined post treatment displayed similar level of Bcl2 phosphorylation to the control group.

Study suggested that inhibition of JNK (Fig. 7M and N) in association with activation of PP2A possibly (Fig. 7O) regulated dephosphorylation of Bcl2 during the 30 days of post treatment with SAC and particularly berberine as well as combined group. The observation was further strengthened after JNK and PP2A inhibitor treatment (Fig. 7K and L). 30 days treatment with SP600125, the potential inhibitor of JNK, attenuated phosphorylation of Bcl2 in the carcinogen exposed group. Again 7 days treatment with okadaic acid, effective inhibitor of PP2A increased the level of pBcl2 in the DEN + CCl4 exposed mice. Since 60 days of post treatment and co-treatment retained Bax concentration towards normal level (Fig. 7C) thus reduction in JNK activity (Fig. 7M and N) and PP2A activation (Fig. 7O) perhaps did not play any significant role in the modulation of Bcl2-Bax interaction (Fig. 7E and G) in the respective groups.

3.7. Modulation of proapototic and antiapoptotic proteins in the liver of DEN + CCl4 exposed mice after SAC and berberine as well as antioxidant inhibitor treatment

It is reported that expression of Bax is upregulated by the tumor suppressor protein p53 [54]. Here our data showed recovery of p53 protein after 30 days of SAC-, berberine- and most significantly in the combined treatment (Fig. 8A and B). Data provided the explanation for the increased expression of Bax in the post treated group specifically after 30 days of treatment (Fig. 7C and D). 60 days of combined treatment and next 10 days without any exposure to the drugs represented retrieval of p53 (Fig. 8A and B) along with reduction in Bax (Fig. 7C and D) and Bcl2 expression (Fig. 7A and B) which were probably correlated with the regaining of normal control cells. Co-treated groups demonstrated insignificant changes in the p53 expression during SAC-, berberine- and combined treatment (Fig. 8A and B) with respect to control. Status of the other antiapoptotic and proapoptotic proteins such as Bcl-xL, PUMA and Bak was analysed. Bcl-xL is the antiapoptotic member of the Bcl-2 family and plays an effective role in the HO1 mediated cytoprotection. Data suggested increased expression of Bcl-xL in the carcinogen exposed group (Fig. 8C and D). Individual SAC, combined and particularly berberine effectively downregulated Bcl-xL expression after 30 days post treatment. Treatment continuation with the combined drug exhibited similar level of Bcl-xL expression in comparison to control animal (Fig. 8C and D). PUMA is a proapototic protein and plays an effective role in tumor suppression by inducing apoptosis. In significant change was observed between control and DEN + CCl4 exposed group though expression of PUMA was significantly reduced in the co treated groups after SAC, berberine and combined treatment (Fig. 8C and E). Since JNK1/c-Jun pathway, but not p53, appears to be responsible for PUMA induction after DEN exposure [55] thus inhibition of pJNK by the SAC and berberine reduced PUMA expression in the DEN + CCl4 exposed co treated group. However in the post treated group PUMA expression remained high in berberine and particularly in the SAC and combined drug treated group with respect to carcinogen exposure. Recovery of p53 in the post treated group probably modulated PUMA expression leading to induction of apoptosis. Another 30 days treatment with combined drug did not display any significant change

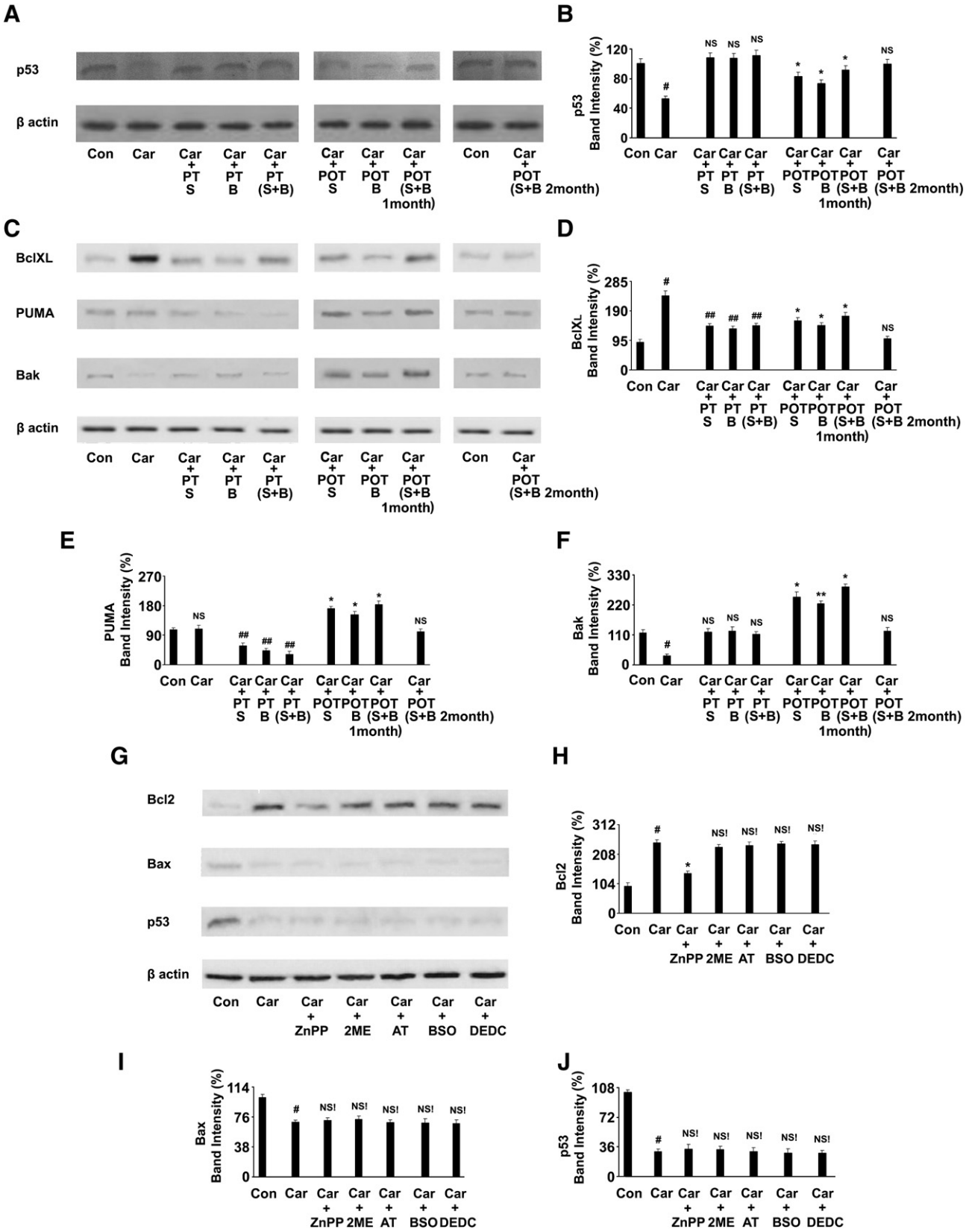

Fig. 8. SAC and berberine treatment modulates the expression of p53, antiapoptotic $Bclx_L$ and proapototic PUMA, Bak expression. Effect of antioxidant inhibitors upon proapototic-antiapoptotic homeostasis was analyzed. Hepatocytes isolated from control, carcinogen exposed and SAC, berberine treated group were lysed in RIPA buffer. Cell lysates were separated by SDS-PAGE and protein expressions were assessed by using respective antibodies; such as (A) antip53, (C) anti $Bclx_L$, anti PUMA, anti Bak. Analysis of β actin was performed as loading control. Densitometric analysis of respective immunoblots of p53 (B), $Bclx_L$ (D), PUMA (E) and Bak (F). (G) DEN + CCl4 exposed mice were treated with ZnPP (HO1 inhibitor), 2ME (MnSOD inhibitor), AT (catalase inhibitor), BSO (γ-glutamylcysteine synthetase inhibitor) and DEDC (CuZnSOD inhibitor). Protein expression of Bcl2, Bax and p53 was analysed. Densitometric analysis of respective immunoblots of Bcl2 (H), of Bax (I) and of p53 (J) were represented. Results are the mean ± SD of five independent experiments (n = 4). NS, ##$p < 0.05$ and #$p < 0.01$ vs. age matched control group; NS!, **$p < 0.02$ and *$p < 0.01$ vs. carcinogen group. PT = Co-treated; POT = Posttreated; S = SAC treated; B = berberine treated and S + B = SAC + berberine treated group.

against control mice. Bak is another important apoptotic protein and plays a significant role in the induction of intrinsic pathway of apoptosis. Data displayed reduced expression of Bak after carcinogenic exposure (Fig. 8C and F). After 30 days of post treatment band intensity was quantitatively increased in berberine and most significantly in SAC and combined drug treated group. 60 days of combined treatment and co treated groups demonstrated insignificant change in Bak expression with respect to control mice.

Next we wanted to study the impact of antioxidants inhibitors on the DEN + CCL4 exposed mice as because accumulated ROS plays a role in the DEN and CCl4 induced hepatocarcinoma. Carcinogen exposed mice were treated with zinc protoporphyrin (ZnPP, HO1 inhibitor); 2methoxy estradiol (2ME, MnSOD inhibitor); N-N′-diethyldithiocarbamate (DEDC, CuZnSOD inhibitor); L-buthionine sulfoximine (BSO, γ-glutamylcysteine synthetase inhibitor); 3-amino-1,2,4-triazole (AT, catalase inhibitor) (Fig. 8G-J). Data suggested only a reduction in the Bcl2 expression (Fig. 8G and H) while p53 (Fig. 8G and J) and Bax (Fig. 8G and I) expression remained unaltered after ZnPP treatment in the DEN + CCl4 exposed group. No significant change was observed in Bcl2, Bax and p53 expression in any other treated groups (Fig. 8G–J). Thus result indicated that only HO1 plays a role in the development of DEN + CCl4 exposed hepatocarcinoma by modulating the expression of antiapoptotic protein Bcl2.

3.8. SAC and berberine treatment modulated HDAC1 and Akt activities in the liver of DEN + CCl4 exposed mice

Nitrosamine induced stress and DNA damage encourages p53 accumulation within nucleus. Thus revival of p53 after SAC and berberine treatment instructed us to analyze the level of nuclear p53 in the carcinogen exposed and drug treated group. Fig. 9A displayed noteworthy reduction in nuclear p53 level in the DEN + CCl4 exposed group with respect to control animal. In commensurate to the total p53 retrieval, result suggested significant accumulation of p53 in the nucleus after 30 days of post treatment with berberine, SAC and particularly the combined drug against carcinogen exposed group (Fig. 9B). Co treatment and 60 days of post treatment with combined drug exhibited control level of p53 within nucleus. Inhibition of deacetylation promotes p53 stability, suggesting that acetylation plays a positive role in the accumulation of p53 protein and assists in mounting the stress response [56]. To resolve the effect of SAC and berberine on the modulation of p53 deacetylation, we determined the acetylated form of p53 within nuclear extract by immuno-blot analysis (Fig. 9A). Densitometric normalization of acetylated p53 with respect to nuclear p53 and the ratio between acetyl p53 and nuclear p53 was depicted in Fig. 9C. Data suggested that reduced p53 acetylation was associated with DEN + CCl4 exposure. Immuno-detection exhibited significant increase in p53 acetylation in parallel to the accumulation of nuclear p53 within post treated groups after 30 days of treatment (Fig. 9A and C). Further analysis of post treated groups suggested that p53 acetylation in the combined group was increased 10.84% ($p < 0.05$) from SAC and 19.49% ($p < 0.02$) from berberine treatment. Extension for another 30 days with a gap for 10 days indicated that degree of p53 acetylation in the SAC + berberine combined group was almost to the control level (Fig. 9A and C). Co-treatment with SAC-, berberine- and the combined drug considerably maintained p53 acetylation in the hepatocytes of DEN + CCl4 exposed mice (Fig. 9A) and the value was more or less similar with the control mice (Fig. 9C). Nuclear fractions were also blotted against β actin to confirm that the nuclear extracts were successfully separated (Fig. 9A). Since dominant-negative HDAC1 mutant promotes both p53 acetylation and stability [57], our next attempt was to assess the activity of HDAC1 in hepatocytes of DEN + CCl4 exposed mice after SAC and berberine treatment. As shown in Fig. 9D, exposure with carcinogen markedly increased the enzymatic activity in nuclear fraction, an effect that was reversed by specifically SAC and in the combined group. Activity of HDAC1 in the combined group was reduced 33.22% ($p < 0.01$) with respect to SAC and 60.48% ($p < 0.01$) was reduced against berberine treatment. Treatment for another 30 days with combined drugs further reduced the HDAC1 activity in the nuclear fraction. Co-treatment with SAC-, berberine-, and in combination also attenuated the enzyme activity within nucleus of the hepatocytes.

HDAC1 binds Mdm2, a negative regulator of p53 and deacetylates the protein at all known acetylated lysine residues leading to ubiquitylation of the protein [57]. Thus we want to analyse Mdm2-HDAC1 interaction by measuring co-immunoprecipitation of pMdm2 against HDAC1 to assess the involvement of Mdm2 in HDAC1 mediated deacetylation of p53 which is required for its degradation. Before the co-immunoprecipitation analysis, HDAC1 (Fig. 9E and F) and pMdm2 (Fig. 9E and G) levels were determined in nuclear extracts of the samples. Co-immunoprecipitated pMdm2 level was normalized with HDAC1 and values were represented in the Fig. 9H. Data showed increased expression of HDAC1 (Fig. 9E and F) and pMdm2 (Fig. 9E and G) in the carcinogen exposed group. It was supported by the significant co-immunoprecipitation of pMdm2 Ser166, an activated form of Mdm2 with HDAC1 and that revealed increased interaction of pMdm2 with HDAC1 in the carcinogen exposed group (Fig. 9E and H). While pMdm2 content and HDAC1 level were decreased notably in all post treated groups (Fig. 9E-G). As a result significant reduction in pMdm2 co-immunoprecipitation with HDAC1 was observed after 30 days of post treatment with SAC, berberine and combined drug (Fig. 9E and H). In the combined group HDAC1/pMdm2 coimmunoprecipitation (Fig. 9E and H) was decreased 14.81% ($p < 0.05$) from SAC and 7.035% (nonsignificant) from berberine post treatment. Not any significant changes were observed in the pMdm2, HDAC1 level and in succession pMdm2 co-immunoprecipitation with HDAC1 in the co-treated and 60 days of post treated groups with respect to control mice (Fig. 9E-H). Further investigation on the total pMdm2 present in whole cell extract also showed enhanced level of pMdm2 in DEN + CCl4 exposed group. The quantity of pMdm2 was down-regulated in post treated groups after SAC-, berberine and combined drug treatment (Fig. 9I and K). pMdm2 level in the post treated combined group was decreased 13.36% ($p < 0.05$) from SAC and 9.61% ($p < 0.05$) against berberine treatment. Band intensity in the co treated groups was similar to the pMdm2 level in control hepatocytes (Fig. 9K). As total Mdm2 level was alike in control, carcinogen exposed, post and co treated group (Fig. 9I and J) therefore we hunted for the reason of increased Mdm2 phosphorylation after DEN + CCl4 exposure. In view of the fact that Akt enhances the ubiquitylation-promoting function of Mdm2 by increasing its phosphorylation, which results in reduction of p53 protein [58], we next examined the effect of DEN + CCl4 exposure on the pAkt level in hepatocytes. Fig. 9L showed increased content of pAkt (pSer473 and pThr308) in the carcinogen exposed group and a noteworthy diminution in SAC and mostly in berberine- and combined group during 30 days of post treatment period. Treatment for another 30 days with combined drug SAC + berberine and a successive gap of 10 days showed more or less same level of pAkt with respect to control group. In co-treatment an insignificant change was observed in the SAC treated group but berberine and the combined treatment displayed to some extent reduction in pSer473Akt level with respect to control animal (Fig. 9L and N). Although pThr308Akt analysis indicated insignificant change in SAC-,berberine- and combined drug treated group (Fig. 9L and M) against control mice. Study suggested increased Akt expression in the carcinogen exposed group (Fig. 9O). As a result more Akt was available for the phosphorylation mediated activation as already observed in the immunoblot analysis of pSer473Akt and pThr308Akt (Fig. 9L-N). In the post treatment particularly berberine and combined drug and also individual treatment with SAC significantly reduced Akt expression against carcinogen exposed group (Fig. 9L and O) and that eventually regulated the reduced level of pAkt (pSer473 and pThr308) in the treated mice (Fig. 9L–N). In the co treatment reduction of pSer473Akt level in the berberine and combined drug (Fig. 9L and N) could be explained by the decrease in Akt expression after berberine and combined drug treatment of

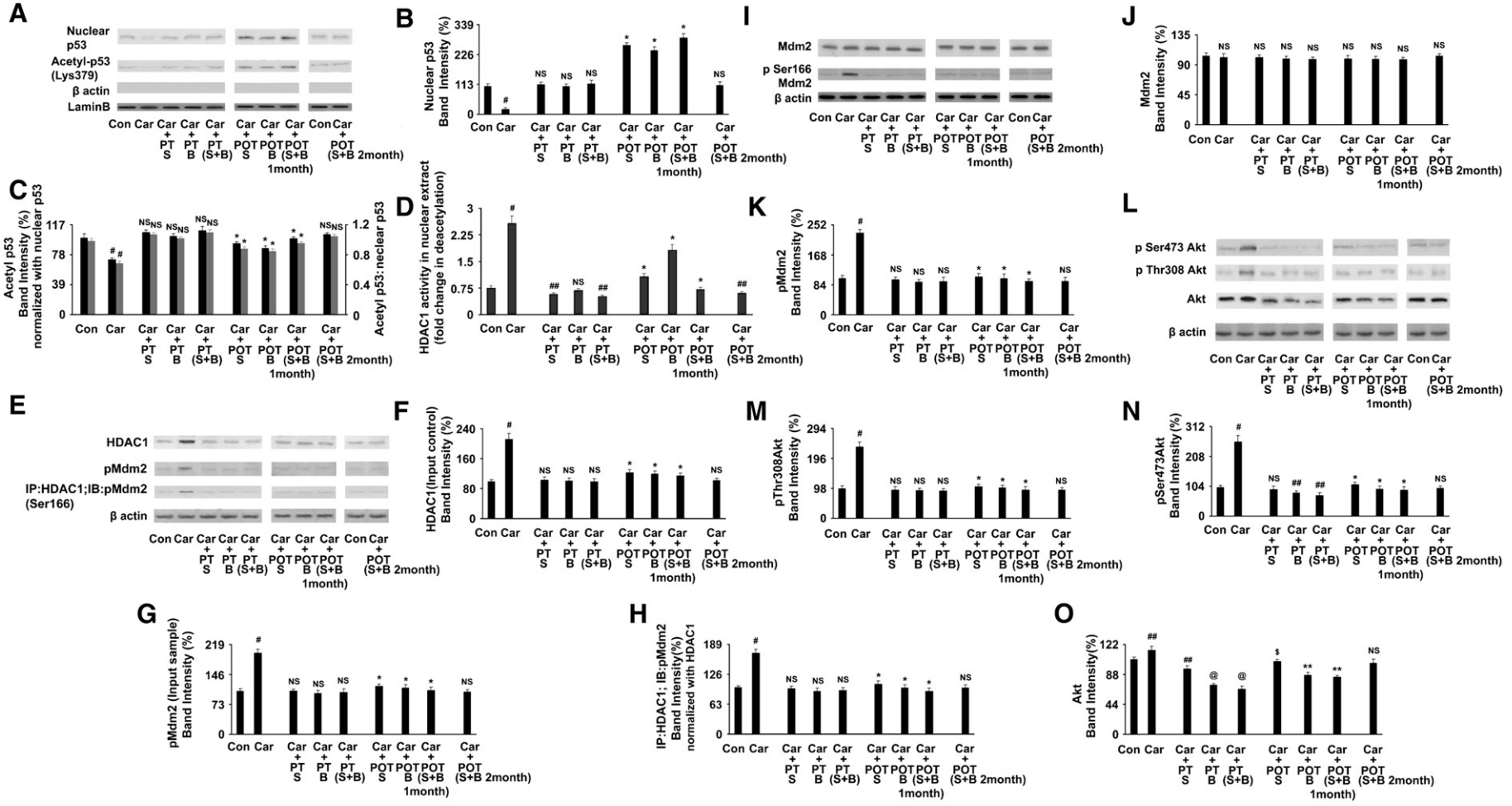

Fig. 9. SAC and berberine treatment inhibit Akt and HDAC1 activities within hepatocytes of DEN + CCl4 exposed mice. Nuclear fraction was separated from cell lysate of control, carcinogen exposed and drug treated group. SDS-PAGE followed by immuno blot analysis using p53 and acetyl-p53 antibody demonstrated change in the p53 acetylation (A) after drug treatment. (D) HDAC1 was immunoprecipitated with anti-HDAC1 antibody and then its activity in control, carcinogen exposed group and SAC, berberine treated group was estimated using HDAC activity assay kit from Cayman Chemical as described in the Materials and methods section. Outcome of reactivity was calculated spectrofluometrically in terms of deacetylation of the substrate after incubation for 30 min at 37 °C. (E) Nuclear extracts of control, carcinogen exposed and SAC, berberine treated groups were immunoprecipitated against anti-HDAC1 and subsequent immuno blot analysis was executed using anti-pMdm2 Ser166 antibody. HDAC1 and pMdm2 level were estimated by using anti HDAC1 and anti pMdm2 antibody respectively before precipitation. (I) Total cellular protein was separated in SDS-PAGE from whole cell extract and expression pattern of Mdm2, pMdm2 Ser166 was assessed after immunoblot analysis. Cell lysate of control, carcinogen exposed and drug treated group were immunoprobed with anti pAkt Ser473, anti pAkt Thr308, anti Akt antibodies on nitrocellulose membrane and prototypes were displayed in (L). Blot against anti-β-actin provided as loading control. Densitometric analysis of respective immunoblots of nuclear p53(B), acetylated p53 in nuclear fraction, normalized with nuclear p53 (C), of nuclear HDAC1(input control) (F), of nuclear pMdm2 (input sample) (G), of Mdm2 (J), of IP: HDAC1 and IB: pMdm2 in nuclear fraction, normalized with HDAC1 (H), of pMdm2 present within whole cell extract (K), pThr308Akt (M), of pSer473Akt (N) and of Akt (O) within total cellular protein were represented. Results are the mean ± SD of five independent experiments (n = 4). NS, ##p < 0.05, @p < 0.02 and #p < 0.01 vs. age matched control group; NS!, $p < 0.05, *p < 0.01 and **p < 0.02 vs. carcinogen group. PT = Co-treated; POT = Posttreated; S = SAC treated; B = berberine treated and S + B = SAC + berberine treated group.

the DEN + CCl4 exposed mice (Fig. 9L and O). Although the impact of reduced Akt expression (Fig. 9L and O) was not reflected in the pThr308Akt level of all co treated groups (Fig. 9L and M) as well as in the pSer473Akt level after SAC co treatment (Fig. 9L and N).

3.9. Dissipation of mitochondrial transmembrane potential and its modification during SAC and berberine treatment in DEN + CCl4 exposed mice

Protein p53 is known to suppress tumor growth, which it does in part by initiating the apoptosis [59]. While it is evident that mitochondrial membrane potential (MMP) plays the decisive role in delimiting the frontier between survival and death [60]. Therefore restoration of p53 instructed us to analyze the status of MMP in the post treated groups after DEN + CCl4 exposure. FACS study (Fig. 10A) indicated higher red to green fluorescence ratio of the JC1, which exhibits potential-dependent accumulation in mitochondria, indicated by a fluorescence emission shift from green (~529 nm) to red (~590 nm), after carcinogen exposure. While 30 days post treatment with SAC + berberine shifted the histogram for green fluorescence towards right and that of red fluorescence towards left (Fig. 10A) indicating significant reduction in concentration-dependent formation of J-aggregates. Administration of single drugs in the post treatment also demonstrated effective reduction in the red to green fluorescence ratio as depicted by Fig. 10B. Additional treatment for another 30 days with combined drug improved the dye retaining capacity as indicated by the rightward shifting of red fluorescence indicating histogram with a simultaneous leftward shifting of green fluorescence signifying histogram. Changes in the red to green fluorescence ratio of JC1 in the co-treated groups were insignificant with respect to control hepatocytes (Fig. 10B).

Similar to mitochondrial depolarization, opening of the MPT pore has been reported to be a responsive mechanism of mitochondrial injury which eventually proceeds to apoptotic death of the cells [61]. Here DEN + CCl4 exposure led to a decrease in the mitochondrial permeability transition from the control level. While SAC-, berberine- and specifically drugs in combination after 30 days of post treatment induced marked increase in the permeabilization of mitochondrial membrane as analyzed from the amplitude of mitochondrial swelling over 7 min. Continuation for further 30 days with the combined treatment although reduced membrane swelling of mitochondria as observed in the Fig. 10D. Consistent with the data of MMP, Fig. 10C exhibited that mitochondrial pore transition remained more or less unchanged in the hepatocytes during SAC and berberine co-treatment in parallel to DEN + CCl4 exposure.

3.10. Effect of SAC and berberine treatment upon cell death regulatory factors in the hepatocytes of DEN + CCl4 exposed mice

Loss of mitochondrial membrane potential induces opening of the MPT pore and thereby releasing intermembrane caspase-activating

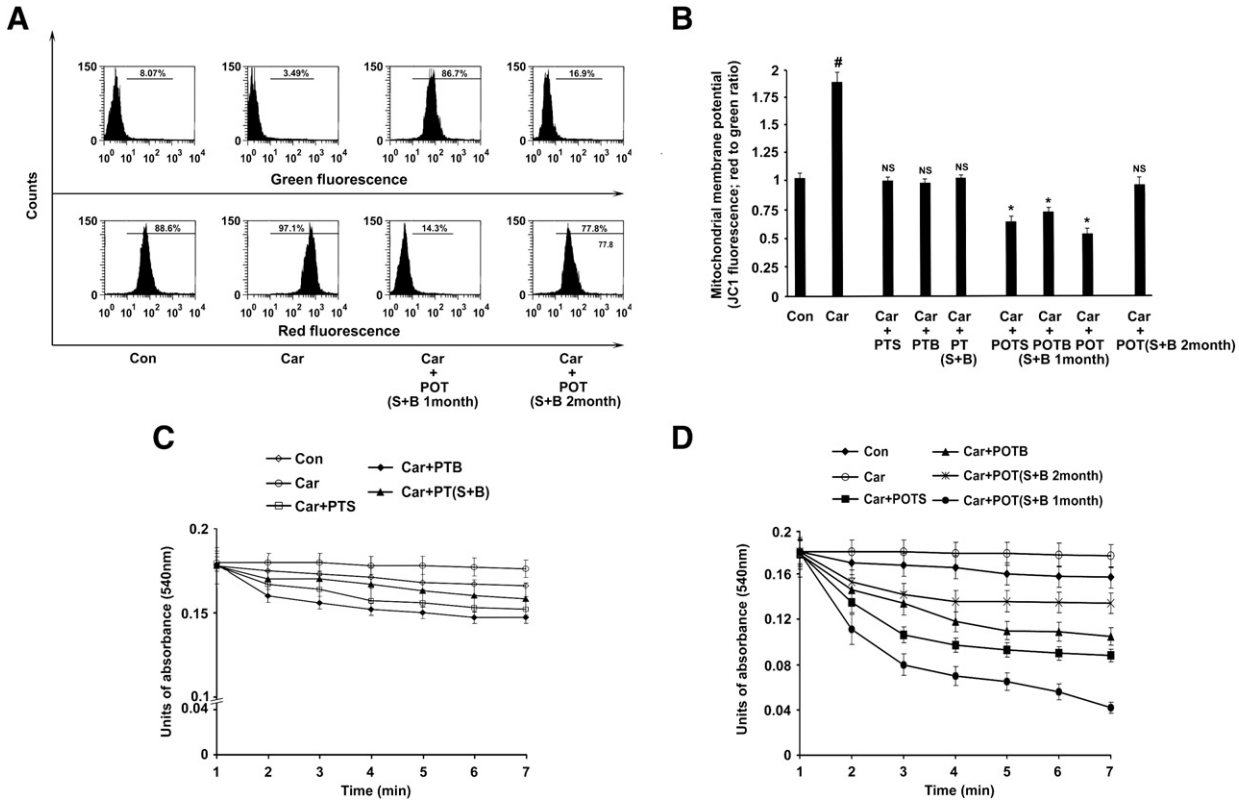

Fig. 10. Impact of SAC and berberine treatment on mitochondrial dysfunction in hepatocytes of DEN + CCl4 exposed mice. Dissipation of MMP was estimated from the calculating red to green fluorescence of JC1 from FACS (A) and fluorimetric analysis (B) as described in the Materials and methods section. DEN + CCl4 exposure increases red fluorescence than control and green fluorescence was reasonably reduced. While green fluorescence was high after 30 days of SAC + berberine treatment indicating greater depolarization of mitochondrial membrane potential with a concommitant decrease in red fluorescence. Continuation of the treatment for another 30 days reduced green fluorescence and significantly increased red fluorescence. Value was progressively reverted back towards control. (B) Fluorimetric determination quantified the red to green fluorescence ratio of JC1 within hepatocytes of control, carcinogen exposed, SAC-, berberine- and combined co- and post treated group. MPT in the hepatocytes was assessed from the changes in amplitude of mitochondrial swelling over time as described in the Materials and methods section. (C) DEN + CCl4 exposure (—○—) reduces the rate of mitochondrial swelling than control (—◇—) and an insignificant change was observed in co-treated groups; such as in PTS (—□—), PTB (—◆—) and PT(S + B) (—▲—). (D) Post treatment for 30 days with SAC (—■—), berberine (—▲—) and most significantly with SAC + berberine (—●—) effectively increases mitochondrial swelling with time. Further continuation of the combined treatment demonstrates (—✳—) increase of absorbance at 540 nm and value was same alike to the control (—◇—). Data are the mean ± SD of five independent experiments (n = 4). NS and #p < 0.01 vs. age matched control group; *p < 0.01 vs. carcinogen group. PT = Co-treated; POT = Post-treated; S = SAC treated; B = berberine treated and S + B = SAC + berberine treated group.

proteins, such as cytochrome C [62]. Our data showed negligible presence of cytochrome C in the cytosolic fraction (Fig. 11A) which was further confirmed by a high ratio of mitochondria to cytoplasmic fraction (Fig. 11C) with a diminished activity of caspase3 (Fig. 11D, E and F) in the hepatocytes of DEN + CCl4 exposed mice. Post-treatment for 30 days of SAC-, berberine-, and SAC + berberine revealed increasing accumulation of cytochrome C in the cytosolic fraction (Fig. 11A) with effective reduction in mitochondria to cytosol ratio specifically in the combined group (Fig. 11C) leading to activation of caspase3 (Fig. 11D, E and F). Extension of the treatment schedule with combined drug for another 30 days reverted back the condition towards control level both with respect to cytosolic cytochrome C accumulation (Fig. 11A) and caspase3 activity (Fig. 11D, E and F). Co-treatment maintained intracellular differential distribution of cytochrome C (Fig. 11A) as evident from the cytosolic immuno blot analysis and quantification in mitochondrial to cytosolic fraction (Fig. 11C) that possibly defined the reason for the

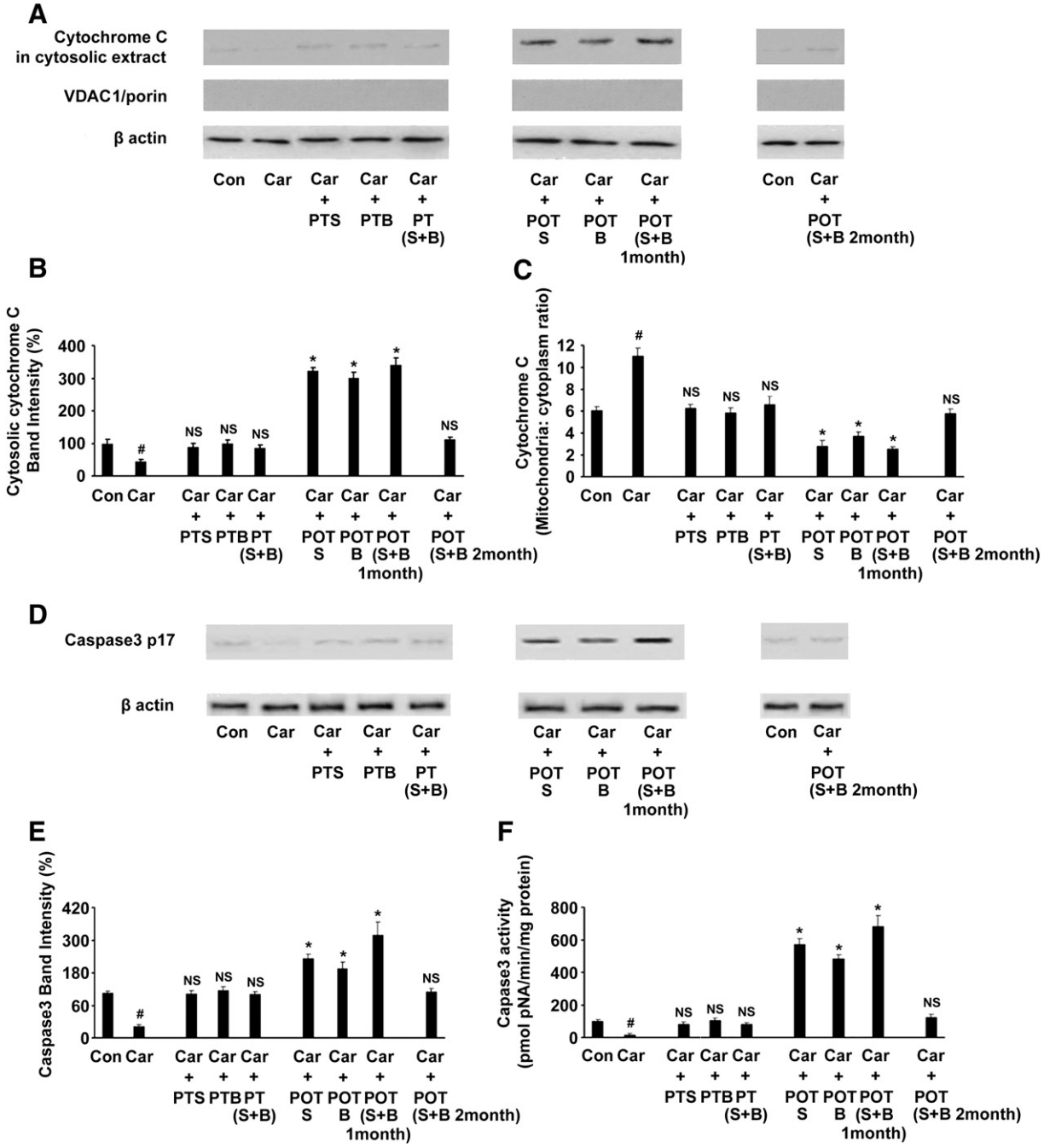

Fig. 11. Role of SAC and berberine treatment on cytochrome C release and caspase3 activation in hepatocytes of DEN + CCl4 exposed mice. (A) Cytochrome C localization in the cytosolic extract of control, carcinogen exposed and SAC, berberine treated group was examined after protein separation in gel electrophoresis followed by immuno blotting with anti cytochrome C antibody. (C) Quantification of cytochrome C within mitochondria and cytosolic extract was performed using Quantikine Rat/Mouse Cytochrome C ELISA from R&D Systems as described in the Materials and methods section. Results are represented in a ratio of mitochondrial to cytosolic content. (D) Whole Cell lysate of the hepatocytes isolated form control, carcinogen exposed and treated group was separated in SDS-PAGE and cleavage of caspase3 was analysed by immuno probing nitrocellulose membrane with caspase3 p17 Antibody. β-actin served as loading control. Densitometric analysis of respective immunoreactive bands such as of cytosolic cytochrome C and of caspase3 was represented in (B) and (E), respectively. (F) Enzymatic activity of Caspase3 was measured using immunosorbent assay. Results are expressed in terms of liberated pNA concentration. Values are the mean ± SD of five independent experiments (n = 4). NS, #p < 0.01 vs. age matched control group; *p < 0.01 vs. carcinogen group. Results are representative of four independent observations. PT = Co-treated; POT = Post-treated; S = SAC treated; B = berberine treated and S + B = SAC + berberine treated group.

maintenance of caspase3 activity (Fig. 11D, E and F) resembling to the control mice.

3.11. Apoptotic regulation of the hepatocytes of DEN + CCl4 exposed mice after SAC, berberine and antioxidant inhibitor treatment

Considering the result presented above, we investigated the extent of phosphatidylserine (PS) externalization on the membrane of hepatocytes before and after the post treatment as well as in co-treatment with SAC and berberine. Simultaneously liver cell necrosis was also estimated because carcinogenic exposure can induce necrosis leading to initiation of the over-proliferation of liver cells that plays a role in the progressive development of hepatocellular carcinoma. Fig. 12A showed significant decrease of annexinV binding (82.6% reduction with respect to control) in the DEN + CCl4 exposed group, which increased effectively with SAC- (21.77%), berberine- (18.5%) and most efficiently in the combined group (29.22%) after 30 days of post treatment (Fig. 12A and B). Further analysis after another 30 days of combined treatment showed reversal of PS externalization and value was almost near to the control level (8.19%). Insignificant changes in the cell death were observed during SAC- (5.69%), berberine- (7.58%) and combined co-treatment (5.12%) with respect to hepatocytes isolated from control animal- (6.33%) (Fig. 12B). PI fluorescence indicated that 0.95% cells were necrotic in the carcinogen exposed group while 0.161% necrotic cells were present in control animal (Fig. 12A). FACS quadrant analysis suggested 1.836%, 1.393% and 2.268% cells were necrotic after 30 days of post treatment with SAC, berberine and combined drug, respectively. Result also suggested that 0.129% cells were necrotic in SAC, 0.186% cells were necrotic in berberine and 0.105% necrotic cells were present in the combined co treated group.

Fig. 12C demonstrated that treatment with HO1 inhibitor significantly and MnSOD inhibitor to some extent increased apoptosis in the liver cells of DEN + CCl4 exposed mice. A minute increase in annexinV-FITC fluorescence was observed in the γ-glutamylcysteine synthetase inhibitor treated group. Data indicated antiapoptotic function of HO1 which probably play a role in the establishment of hepatocarcinoma after DEN + CCl4 exposure.

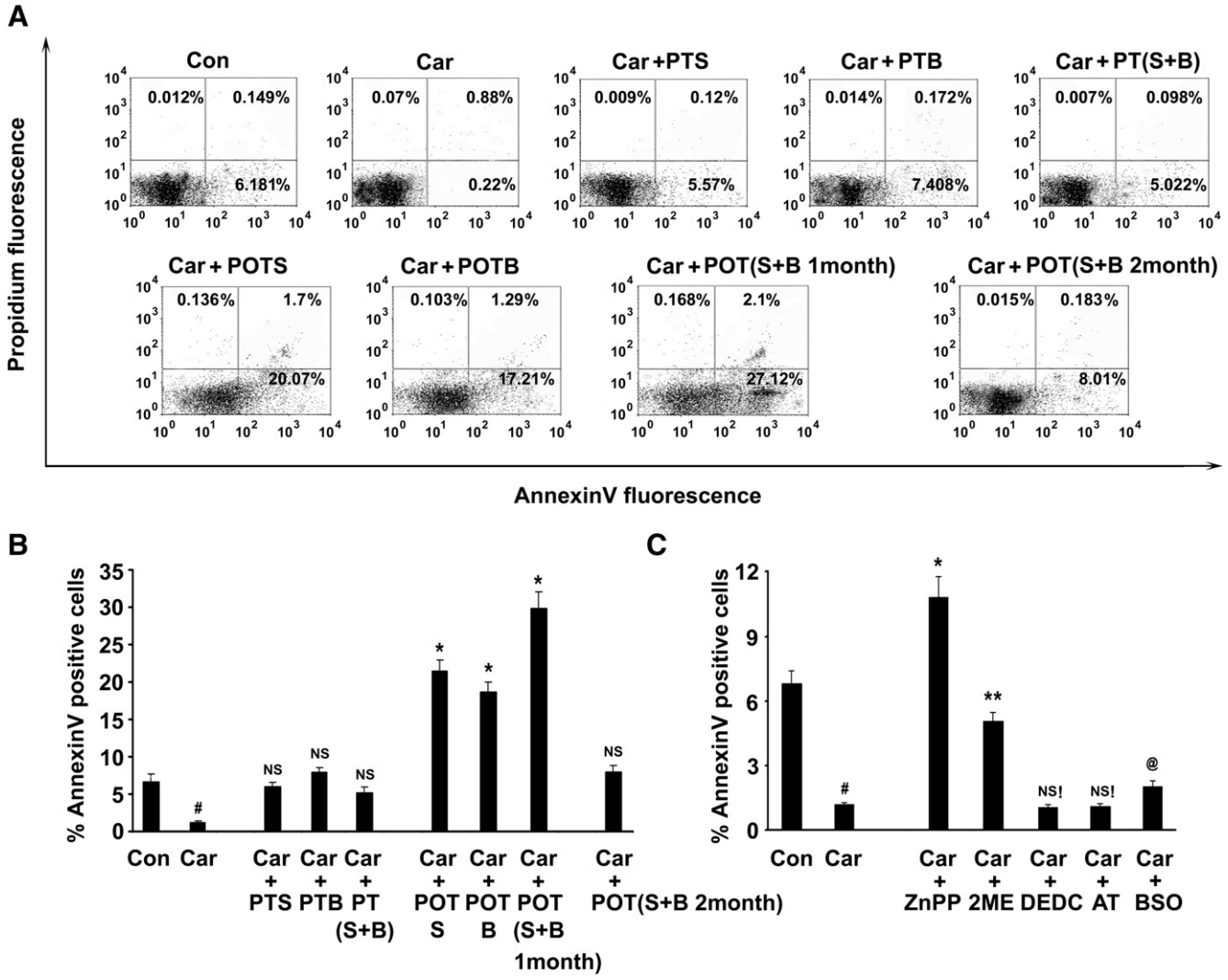

Fig. 12. Impact of SAC, berberine and antioxidant inhibitor treatment on the apoptosis of hepatocytes isolated from DEN + CCl4 exposed mice. (A) 5×10^7 hepatocytes of control, carcinogen exposed and drug treated group were incubated with 1 μg/ml FITC-labeled annexinV and 1 μg/ml PI. Subsequent flow cytometric estimation analysed the percentage of apoptotic and necrotic cells. Numbers in the lower right quadrate indicated percentage of early apoptotic cells, upper left quadrate of necrotic cells and upper right quadrate indicated the percentage of annexinV as well as PI positive cells in the respective samples. (B) Percentage of annexinV positive cells present in the liver of control, carcinogen exposed, post as well as co-treated groups were analysed. Values were represented in histogram.(C) Impact of antioxidant inhibitors such as ZnPP (HO1 inhibitor), 2ME (MnSOD inhibitor), AT (catalase inhibitor), BSO (γ-glutamylcysteine synthetase inhibitor) and DEDC (CuZnSOD inhibitor) upon liver cell apoptosis of DEN + CCl4 exposed mice. Treatment procedure was described in details in the Materials and methods section. Results are representative of four independent observations. NS, #$p < 0.01$ against control mice and NS!,*$p < 0.01$,**$p < 0.02$,@$p < 0.05$ against carcinogen group. PT = Co-treated; POT = Post-treated; S = SAC treated; B = berberine treated and S + B = SAC + berberine treated group.

3.12. Analysis of the effect of SAC and berberine treatment on DEN + CCl4 exposure by representing liver histology and tunnel assay

Histological studies illustrated the presence of hyperchromic pleomorphic nuclei containing dysplastic hepatocytes (marked with white arrow) associated with inflammatory cell cluster (marked with black arrow) in the DEN + CCl4 exposed mice (Fig. 13A). Section predominantly with larger nucleus indicated high mitotic activity and that possibly helped in the cell growth and proliferation during DEN + CCl4 exposure. 30 days of post treatment with SAC + berberine reduced the number of dysplastic hepatocytes (marked with white arrow) with concomitant increase in the number of apoptotic cells (marked with black arrow) (Fig. 13A). But continuation of the combined treatment for 30 days with a break of 10 days was noticeable in the company both of a decreased number of apoptotic cells as well as dysplastic hepatocytes (Fig. 13A). Co-treatment with SAC + berberine protected cells from any such deformations mediated by DEN + CCl4 as evident by the histological analysis (Fig. 13A).

In addition to the histological analysis tunnel assay was performed for in situ analysis of apoptosis (Fig. 13B). Considerable DNA fragmentation was observed after 30 days of SAC + berberine treatment (marked by white arrows in the merged figure). No apoptotic DNA fragmentation was observed in the carcinogen exposed group. While 60 days of combined post treated group and co treated combined group displayed similar features with respect to control animal.

3.13. SAC and berberine responsible for amelioration of DEN + CCl4 induced hepatocarcinoma

To confirm the role of SAC as HDAC1 inhibitor and that of berberine as a potential Akt inhibitor in the amelioration of DEN + CCl4 induced hepatocarcinoma, carcinogen exposed mice were treated with α-tocopherol the anti-oxidant, Akt inhibitor triciribine and HDAC1 inhibitor trichostatin A individually or in combination for a total period of 60 days similar to the SAC + berberine treatment schedule. Fig. 14 demonstrated reduction in PCNA expression (value was normalized against loading control and represented as % of control) after trichostatin A and triciribine individual treatment. The value was only comparable to SAC + berberine when the animals were treated with α-tocopherol + triciribine + trichostatin A in a combined form. Again dysplastic to normal cell ratio were most efficiently diminuted in the α-tocopherol + triciribine + trichostatin A treated group and value was equivalent to SAC + berberine treatment as demonstrated in Fig. 14. Treatment with trichostatin A and triciribine together exhibited similar effects in comparison to α-tocopherol + triciribine + trichostatin A combined group. Thus figure pointed out that HDAC1 and Akt inhibitory property of SAC + berberine mostly played a significant role to ensure an effective protection against DEN + CCl4 induced hepatocarcinoma in mice.

3.14. Biomolecular mechanism of SAC + berberine treatment on the DEN + CCl4 exposed hepatocellular carcinoma

Fig. 15 elucidated biochemical basis of SAC + berberine treatment in mice after DEN + CCl4 exposure. According to our data CYP2E1 mediated activation of DEN + CCl4 induced the accumulation of ROS within the hepatocytes (Fig. 4G) due to impaired function of anti-oxidant system (Fig. 5). ROS mediated activation of Nrf2-HO1 pathway (Fig. 6) further stimulated proapoptotic Bcl2 expression (Fig. 7A and B). JNK dependent Bcl2 phosphorylation (Fig. 7H, J, K and L) in turn encouraged its interaction with residual Bax which was reduced in expression in the carcinogen exposed group. Moreover, result showed that bio-active DEN + CCl4 promoted Akt dependent Mdm2 phosphorylation (Fig. 9I and K) that finally formed a complex with HDAC1 (Fig. 9E and H). This complex probably regulated p53 deacetylation within nucleus which was in accordance with the prior report [53]. p53 deacetylation was well accompanied with p53 degradation (Fig. 8A and B; Fig. 9A and B) leading to downregulation of Bax, as observed in the

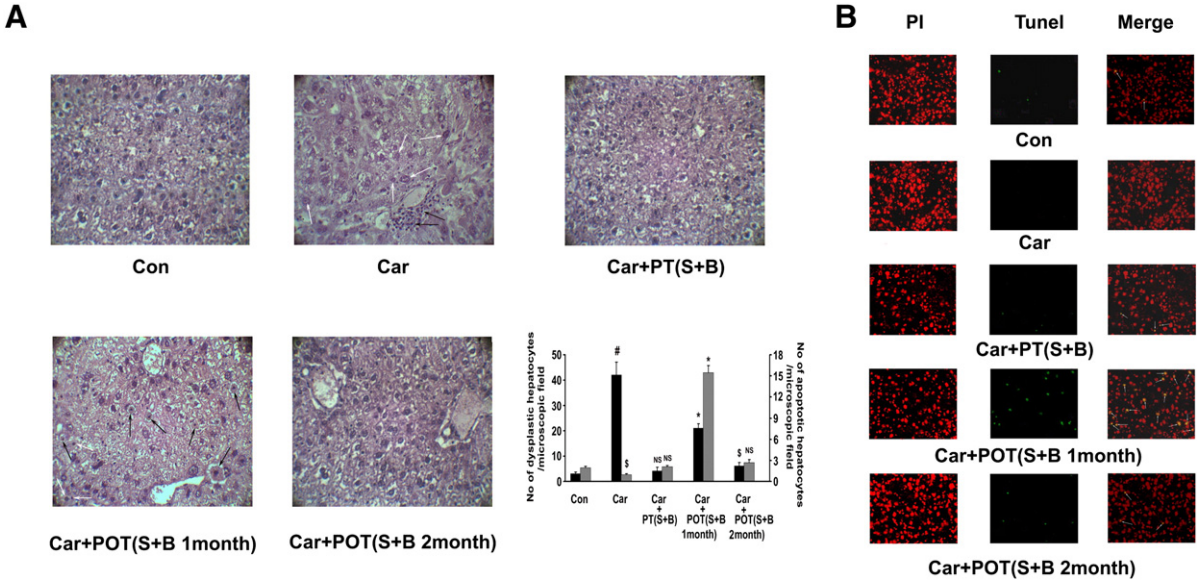

Fig. 13. Histological study of the liver tissue obtained from DEN + CCl4 exposed and SAC + berberine treated experimental groups. Representative H&E-stained liver sections of five independent observations were photographed at 400× magnification. (A) Control group demonstrated a structured homomorphic architecture with distinctly arranged hepatocytes. DEN + CCl4-induced animals showed hyperchromic anisonucleosis in association with cellular dysplasia (indicated by white arrows), loss of architecture and inflammatory cell cluster (indicated by black arrows). Animals co-treated with SAC + berberine revealed normal architecture. Post treatment with SAC + berberine pointed towards the presence of several apoptotic hepatocytes (indicated by black arrows) with some pleomorphic nuclei (indicated by white arrows). Continuation of the treatment with combined drug demonstrated normal tissue structure. Numbers of dysplastic and apoptotic hepatocytes were calculated in control, carcinogen exposed and drug treated group by counting the cells in 10 microscopic fields from liver sections of each of the animal of each experimental group with a 40× objective. Average number of cells per field of the individual groups was represented in histogram. (B) In situ apoptotic analysis was performed by Tunnel assay. Tunnel positive nuclei were visualized by FITC-dUTP staining (middle panel) and DNA by PI (left panel). In the merged figure (right panel) fragmented apoptotic DNA was marked by white arrows. High DNA fragmentation was observed in the 30 days of combined post treated group. Continuation of treatment reduced the DNA fragmentation as demarcated by white arrows. Values were represented in a ratio of dysplastic to control hepatocytes. Data are the mean ± SD of five independent experiments (n = 4). NS,#p < 0.01 and $p < 0.05 vs control group and *p < 0.01 vs carcinogen group. PT = Co-treated; POT = Post-treated; S = SAC treated; B = berberine treated and S + B = SAC + berberine treated group.

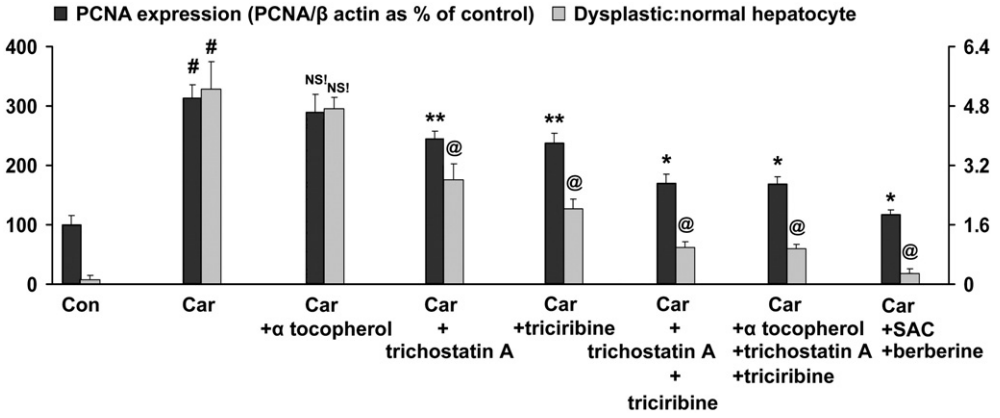

Fig. 14. Analysis of SAC and berberine properties responsible for effective amelioration of DEN + CCl4 induced hepato carcinoma. After 60 days exposure of DEN + CCl4, animals were treated with α tocopherol as a potential anti-oxidant (200 mg/kg bw/day by gavage), trichostatinA as a HDAC1 inhibitor (1 mg/kg bw/day by i.p. injection), triciribine as an Akt inhibitor (1 mg/kg bw/day by i.p. infusion) or in combination for 60 days. The control group received solvent only. PCNA expression was analysed in each of the group and the value was presented as percentage of control after normalizing against loading control β actin. The numbers of dysplastic cells were quantified from H&E-stained liver histology. Cells were calculated by observing 8 microscopic fields from liver sections of each of the animal of each experimental group under 40× objective. Values were represented in a ratio of dysplastic to normal hepatocytes. Data are the mean ± SD of five independent experiments (n = 4). #$p < 0.01$ vs. age matched control group; NS!, $^{**}p < 0.02$, @$p < 0.02$ and $^{*}p < 0.01$ vs. carcinogen group. PT = Co-treated; POT = Post-treated; S = SAC treated; B = berberine treated and S + B = SAC + berberine treated group.

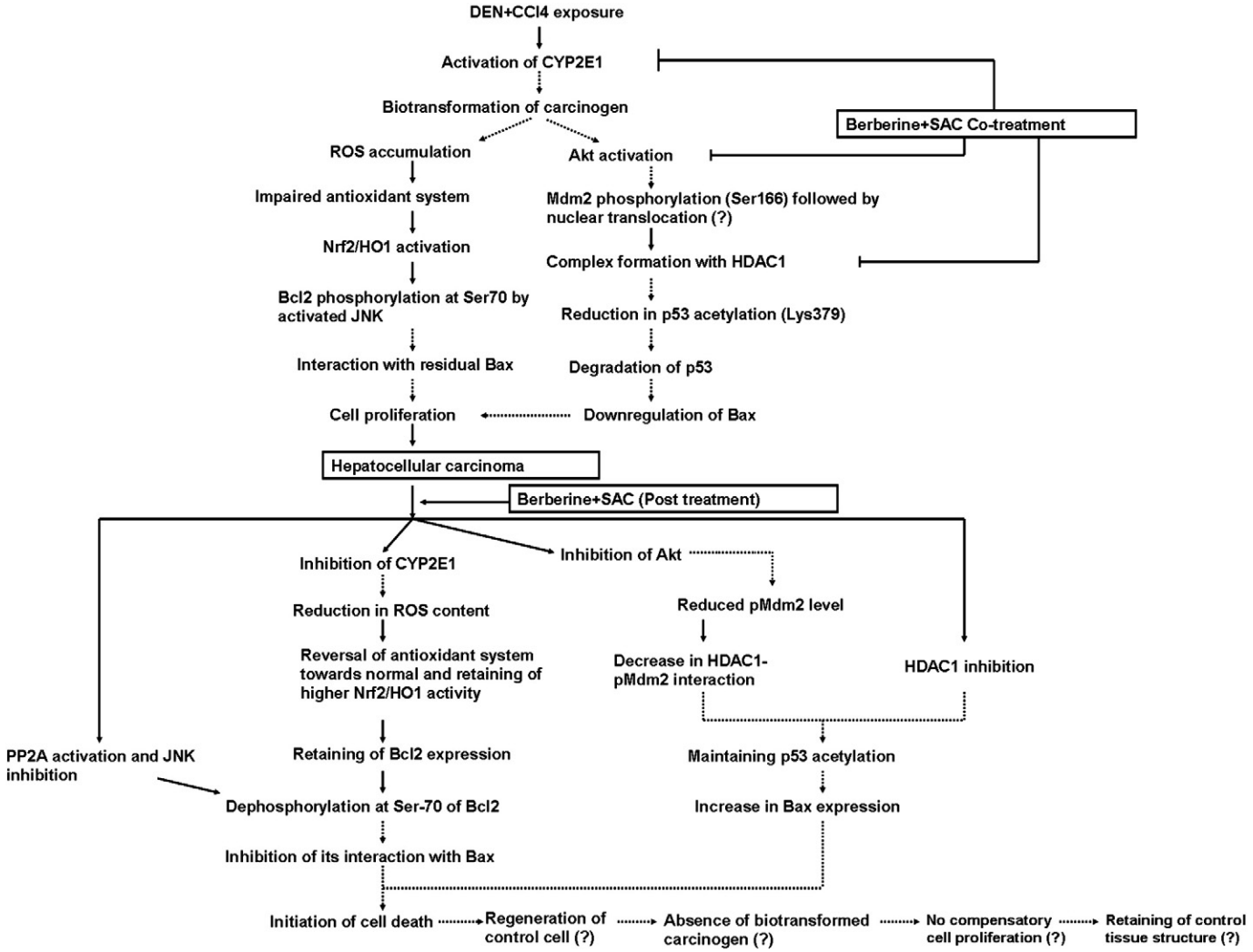

Fig. 15. Probable schematic representation of the DEN + CCl4 mediated bio-physiological modulation leading to development of hepatocarcinoma. Target molecules for SAC and berberine were demarcated in the drug treated group. Mechanisms of SAC and berberine mediated apoptosis in hepatocytes of DEN + CCl4 exposed mice during post treatment for 30 days were delineated. Lay out proposed the importance of the absence of compensatory proliferation in the maintenance of normal tissue structure.

DEN + CCl4 exposed group (Fig. 7C and D). Thus simultaneous Bcl2 over-expression, increased phosphorylation and Bax downregulation paved the pathway of cell proliferation leading to hepatocarcinoma.

Berberine + SAC inhibited CYP2E1 activity (Fig. 4F), reduced oxidative stress (Fig. 4G) by retaining the antioxidant system (Fig. 5) and Nrf2-HO1 activity (Fig. 6) that led to maintenance of Bcl2 expression (Fig. 7A and B). Treatment with drugs also reduced pMdm2 formation (Fig. 9I and K) by inhibiting Akt (Fig. 9L, M and N) and simultaneous HDAC1 inhibition (Fig. 9D) maintained p53 acetylation (Fig. 9A and B) with an increase in Bax expression as demonstrated by Fig. 7C and D. Moreover PP2A activation (Fig. 7O) in association with JNK inhibition (Fig. 7M and N) dephosphorylate Bcl2 (Fig. 7H, J, K and L) and eventually inhibited Bcl2/Bax interaction (Fig. 7E and G) in the 30 days of post treatment.

Substantial decrease in Bcl2/Bax heterodimer formation initiated the cell death (Fig. 10, Fig. 11 and Fig. 12) and the resulting void area was probably refilled by control cell. Experimental analysis also indicated restraining of compensatory cell proliferation due to inhibition of biotransformation of carcinogens resulting regaining of control tissue structure as depicted in Fig. 13A.

4. Discussion

Nitrosamines are the compounds with a chemical structure of R1N(-R2)-N O. Under acidic conditions the nitrite forms nitrous acid, which is protonated and splits into nitrosonium cation and water. The nitrosonium cation then reacts with an amine to produce nitrosamine which has potential carcinogenic effect [63,64]. Endogenous nitrosamines can be formed in a similar way from their precursors, nitrates and nitrites, which are present in foods as preservative and are characterized as environmental dietary carcinogen [65]. Even though diet is the main source of exposure, occupational environment such as rubber products and metal industries, leather tanneries, pesticide production, dye manufacturing and fish processing industries also contribute substantially to the high risk of nitrosamine introduction [66]. For these reasons intensive studies are conducted on DEN induced hepatocarcinoma using both rat and mouse as model [67,68].

A number of signaling pathways have been implicated in DEN-induced liver cancinogenesis. Initially rapid killing of hepatocytes is induced by DEN. Since liver is capable of natural regeneration of lost tissue, thus increased hepatocyte death results in a more extensive compensatory proliferative response that enhances the formation of HCC in DEN-exposed mice [69]. DEN by itself requires long time to induce hepatocarcinoma but assistance of tumor promoters ensure shorter time span for the development of liver cancer [70]. Many of the tumor promoters, such as CCl4, which was previously used as a dry cleaning solvent also in refrigeration and lava lamps, enhance hepatocyte proliferation through indirect mechanisms. Essentially their primary effect is cytotoxicity that eventually triggers compensatory proliferation [70,71]. Therefore in our study DEN + CCl4 were used experimentally to demonstrate important molecular and cellular pathways involved in HCC development.

It is reported that inflammation is one of the main factors of the generation and development of liver cancer. The IKK/NF-κB signal pathway regulates various signaling and inflammatory factors, which are related to the effective modulation of liver inflammation and facilitates the development of HCC [72]. Currently different herbal extracts are included in the experimental analysis to examine their hepatoprotective properties. Moreover, considering the cost effective well known benefits, these herbal extracts are hoping to be used either alone or in combination with conventional chemotherapy in order to reduce its side effects [73–75]. *Glossogyne tenuifolia* has been shown to inhibit the release of IFN-γ and IL-6 in LPS-activated PBMC from HCC patients, thus producing anti-hepatocarcinogenic effects [76]. In another study, it has been identified that chloroform extracts of *Terminalia catappa* exerts hepatoprotective effects that might be related to the regulation of liver IL-6 gene expression [77]. Besides, these hepatoprotective drugs may be related, at least in part, in their ability to reduce NF-κB activation [78], indicating their proficiency in the modulation of NF-κB effects on HCC.

Treatment with potential antioxidant curcumin effectively reduced both, tumor multiplicity and incidence of diethylnitrosamine-induced HCC. It is suggested that in *in vivo*, curcumin primarily prevents tumor invasion rather than displaying cytotoxic chemotherapeutic actions [79]. Garlic organosulfur compounds also exert chemo-preventive effects by scavenging free radicals and modulating the role of antioxidant system in liver of carcinogen exposed rodents [80]. Water-soluble sulfur compounds like SAC or SAMC modulate cell proliferation by regulating antioxidant-dependent carcinogen detoxification systems [81]. Effective radical scavenging ability suggests that hepatoprotective mechanism and anti-carcinogenic property of SAC may be attributed to its antioxidant activity.

According to the reports, berberine, another potential free radical scavenger, is able to modulate ROS dependent various biological effects, such as cell proliferation, survival, metabolic activation and apoptosis, by regulating many signaling molecules, such as MAPK, ERK1/2, JNK, NF-kB, Akt, caspases, and calcium. Berberine administration showed inhibitory effects on lipoxygenase and xanthine oxidase, two important ROS-derived sources, that in turn suggests its efficacy as antioxidant. Antioxidative properties of berberine play a significant role in the negative modulation of NF-kB activation, the effector signal of various inflammatory agents and carcinogens, leading to hepatoprotection [82]. The possible mechanism of berberine mediated hepato protection is conducted by the inhibition of CYP enzymes which are responsible for the bioactivation of carcinogenic materials [83].

Study also indicated reduction in the cell proliferation markers after SAC and berberine treatment. Thus present analysis was performed to identify possible target molecules in order to block chemically induced liver carcinogenesis by using hepatoprotective as well as anti-carcinogenic properties of SAC and berberine in *in vivo*.

Reports suggest that DEN is hydroxylated by CYP2E1 in the liver, through an alkylation, to become bioactive. Simultaneous oxidation of α carbon within microsomes induces its DNA damaging activity [49]. Moreover, CYP2E1 has shown to be the principal catalyst for biotransformation of CCl4 into trichloromethyl free radicals [50]. Biometabolism of both DEN and CCl4 ultimately releases high amount of toxic intermediates or ROS. The effects of ROS in carcinogenic nitrosamines and CCl4 mediated hepatic injury are well documented [84,85]. Moreover, impaired antioxidant system, as indicated by the defective functioning of both enzymatic (Cu-Zn-SOD, Mn-SOD and catalase) and non enzymatic (GSH) forms, failed to scavenge generated ROS from CYP2E1 activity within the hepatocytes and contributed to the development of oxidative stress during DEN + CCl4 exposure. Generated oxidative stress is involved in the oxidation of membrane protein and lipids [86] which is in agreement with our result. Increased TBARS value in the DEN + CCl4 exposed group indicated membrane lipid peroxidation leading to destabilization and disintegration of the cell membranes. That eventually released stress specific enzymes in the serum, which was reflected by the marked elevations of liver functional markers such as ALT, AST, LDH and ALKP in the DEN + CCl4 exposed mice. Current reports about the SAC, an active organo-sulfur compound of garlic and berberine, an isoquinoline alkaloid of goldenseal as antioxidant with chemopreventive effects encouraged us to investigate their role in combination in experimentally induced hepatocarcinoma. Our result showed disappearance of gray-white nodular patches from the surface of the liver after 30 days of treatment with the dose of 250 mg/kg body weight of SAC and 8 mg/kg body weight of berberine as decided by analyzing liver function test. Retaining of the normal morphology in the co-treated group specified the effectivity of determined dose of SAC and berberine. Data revealed that combined dose most efficiently reduced CYP2E1 activity and also able to revert-back antioxidant status. This was reflected in the diminution of oxidative stress

as well as in the reduction of TBARS value during 30 days of post treatment with SAC and berberine. Effective inhibition of the CYP2E1 with the maintenance of anti oxidant status by SAC and berberine was manifested by the trivial change in ROS and lipid peroxidation (LPO) in the hepatocytes of co-treated mice.

Accumulation of ROS induces Nrf2/HO1 activity [51,87]. Here imposed oxidative stress by CYP2E1 in association with increased expression of Nrf2 and HO1 in the carcinogen exposed group suggesting an instrumental role of DEN + CCl4 exposure in the activation of Nrf2/HO1 pathway. Data showed increased expression of Nrf2 in the nuclear fraction indicating its possible translocation towards nucleus for transcriptional transactivation of ARE genes. It was further supported by the high expression/activity of HO1 in the DEN + CCl4 exposed mice. Although, Nrf2/HO1 pathway probably finally exhausted in the DEN + CCl4 exposed group, leading to accumulation of more and more ROS. SAC and berberine, the potential antioxidants, individually and more efficiently in combination, reduced ROS accumulation resulting decrease in the expression and eventually the activity of HO1 with respect to exposed mice. But treatment with the drugs (SAC and berberine) somehow maintained Nrf2/HO1 pathway as evident by the keeping of Nrf2 expression and HO1 expression/activity after 30 days of post-treatment with respect to control mice. This was possibly due to carcinogenic induction which increased Nrf2/HO1 pathway to such higher extent that SAC and berberine individually as well as in combination were unable to modulate it towards control level after 30 days of post treatment. Moreover, increased value in Nrf2/HO1 expression/activity in the co-treated group (individual and combined group) with respect to control provided us a rationale for further suggesting the role of antioxidant properties of SAC and berberine in the maintenance of Nrf2/HO1 pathway.

Induction of cytoprotective enzyme heme oxygenase-1 (HO1) has been observed in the cells of renal adenocarcinoma, lymphosarcoma, hepatoma, melanoma and squamous carcinoma that eventually promotes cancer progression [88,89]. Upregulation of HO1 activity catalyzes heme degradation into biliverdin, which is subsequently reduced to bilirubin, free iron and equimolar amounts of carbon monoxide (CO). Generated CO in the said reaction probably mediates anti apoptotic effects of HO1 [90]. Over-expression of HO1 has been reported for the close association with a concommitant increase in the levels of the anti-apoptotic protein Bcl-2 [52,91] which was observed in our studies. Simultaneous decrease in pro-apoptotic protein Bax probably paved the pathway of cell proliferation in DEN + CCl4 exposed group. Experimental analysis with antioxidant inhibitors further demonstrated the anti-apoptotic role of HO1 during chemically induced hepatocarcinoma. Effective reduction in Bcl2 expression after ZnPP (the potential HO1 inhibitor) treatment suggested the significant role of Bcl2 in the establishment of cytoprotective activity of HO1 that led to development of HCC in DEN + CCl4 exposed mice.

Post-treatment for one month with SAC and in combination with berberine maintained the expression of Bcl2 to some extent possibly due to the keeping up of Nrf2/HO1 pathway although the quantitative value of the protein was much lower than the carcinogen exposed group. Experimental analysis in 30 days post treated group indicated significant increase in pro-apoptotic protein Bax concentration. It is reported that cellular homeostatic balance between cell survival and cell death is conducted by Bax/ Bcl2 ratio and any increase in the Bax/Bcl2 heterodimerization ensures cell growth and proliferation [53,92]. Thus co-immunoprecipitation was performed to find out the Bcl2/Bax interaction in the SAC and berberine treatment. Trivial co-immunoprecipitation of Bax with Bcl2 was in accordance with the reduction in Bax concentration in the carcinogen exposed group. While 30 days of SAC and berberine individual and combined post treatment demonstrated significant Bax co-immunoprecipitation with respect to DEN + CCl4 exposure. Although the normalized band intensities of co-immunoprecipitated Bax was downregulated after 30 days of individual and combined drug treatment against control animal. These 30 days SAC and berberine post treated groups were associated with effective high concentration of Bax and a moderate level of Bcl2 which were not reflected in the experimental Bcl2-Bax co-immunoprecipitation. The analysis guided us to evaluate the Ser70 phosphorylation status of Bcl2, the chief regulatory factor for its stable interaction with Bax [53]. Noteworthy increase in Ser70 phosphorylation of Bcl2 prevented residual Bax mediated any modulation in liver cell physiology of DEN + CCl4 exposed group. Reduced Bcl2 phosphorylation in the 30 days of post treated groups potentiated decreased Bcl2-Bax interaction, the probable cause of decreased Bax co-immunoprecipitation with respect to control animal. Thus additional Bax was available to regulate cell metabolism and cell death due to considerable high expression of Bax in the individual and combined 30 days of treatment. Data analysis also suggested a differential Bcl2-Bax interaction among the individual and combined post treated groups. Notable reduction in Bcl2-Bax interaction in the combined group against SAC was probably due to integration of the effect of berberine with individual SAC treatment.

It is reported that JNK has an essential role in HCC development. In JNK1 knockout mice, DEN triggered liver tumorigenesis was remarkably reduced. Treatment with JNK inhibitors resulted in the reduced growth of xenografted human HCC cells [93,94]. Reduced phosphorylated Ser70 Bcl2 level with respect to control suggested the involvement of SAC- and most specifically berberine and combined drug in the inhibition of JNK and PP2A after 30 days of post treatment. Increased JNK activity and a fall in PP2A activity sustained Bcl2 phosphorylation in the carcinogen exposed group.

Both Bcl2 and Bax are transcriptional targets for the tumor suppressor protein p53, the well known key initiator of apoptosis [95]. Moreover studies indicated that carcinogenic DNA damage makes nuclear localization of p53 [96–98] where it effectively modulates the expression of cell death regulatory proteins and directs the cell fate towards apoptosis [95]. Although bio-activation of carcinogens promoted Akt mediated phosphorylation of Mdm2 that in turn probably translocated into the nucleus and formed a complex with HDAC1. HDAC1-pMdm2 complex interacts with p53 resulting deacetylation of the protein [57]. The deacetylated p53 binds poorly to the target promoter (p21), which results in switching off the p53 response, essential for re-entry into the cell cycle [57]. As the acetylated p53 lysine residues overlap with ubiquitylation sites [57] therefore recruitment of HDAC1 by Mdm2 perhaps promoted p53 degradation in the DEN + CCl4 exposed mice. 30 days of post treatment with SAC and berberine reduced pMdm2 level by inhibiting (pSer473 and pThr308 pAkt) pAKT. As a result significant recovery of p53 was observed due to restraining of HDAC1 mediated p53 deacetylation and the event was associated with increased expression of Bax suggesting initiation of cell death.

In the co-treatments discernible inhibition of the CYP2E1 inhibited the production of active carcinogenic biometabolites from DEN and CCl4. Thus the group illustrated expressions of p53, Bax and Bak more or less similar to the control. Drug treatment in parallel to DEN + CCl4 exposure also maintained BCl2/Bax interaction to a basal level in spite of drug dependent considerable high expression of Bcl2 with respect to control animal. The effect possibly explained by the insignificant change in Ser70 Bcl2 phosphorylation due to reduction in JNK and activation of PP2A in co-treated group. Inactivation of JNK also reduced PUMA expression significantly in co-treated group. PUMA, the p53 upregulated modulator of apoptosis, is a pro apoptotic protein and it suppresses the development of tumor by inducing apoptosis. Although JNK1 mediated and p53 independent PUMA upregulation was observed in the DEN exposed mice. As a result apoptotic cell death is initiated and compensatory cell proliferation is induced in the host animal leading to progressive development of HCC. $Bclx_L$, a member of Bcl2 family protein and a downstream effector molecule of HO1 anti apoptotic pathway, acts as a pro survival protein by preventing the release of cytochrome C from mitochondria. Here $Bclx_L$ expression remained higher than control in the co-treated group possibly due to inductive effect of HO1. Bak, the Bcl2 homologous killer, is another pro apoptotic protein and stimulates

the intrinsic pathway by inducing the release of cytochrome C from mitochondria. Similar band intensities to control animal suggested its insignificant role in the in the modulation of HCC in co-treated groups.

DEN + CCl4 exposure effectively increased $Bclx_L$ expression same as to Bcl2. Probably increased HO1 expression played a regulatory role in $Bclx_L$ upregulation in the carcinogen exposed group. While data indicated no significant change in PUMA expression in the DEN + CCl4 exposed group with respect to control. During development of hepatocarcinoma PUMA expression remains high [55]. After the establishment of HCC probably expression of the protein is reverted back to control level to increase cellular life span. Cell survivability was further potentiated by the reduced Bak expression in DEN + CCl4 exposed mice. SAC and berberine reduced $Bclx_L$, increased PUMA and Bak expression after 30 days of treatment. Post treatment recovery of p53 probably stimulated PUMA and Bak expression led to induction of apoptosis.

Fairly high mitochondrial membrane potential with a diminished value of effector caspase3 and reduced exposure of PS on the cell surface in comparison to control demonstrated additional affirmation of cell survival in the DEN + CCl4 exposed group. Collapse of $\Delta\psi m$ as an outcome of permeabilization of the inner mitochondrial membrane [60,99] in conjunction with the opening of MPT influenced the release of cytochrome C in the cytosolic fraction as evident by the decreased mitochondria to cytosolic ratio of cytochrome C in the 30 days of post treated mice. Activation of caspase3 plus increased exposure of PS on the cell surface depicted the efficacy of SAC and berberine in the induction of cancerous cell death after chronic exposure to DEN + CCl4. Maintenance of $\Delta\psi m$ by SAC and berberine co-treatment protected cells from cytochrome C mediated caspase3 activation and PS exposure, the marker of cell death pathway. Moreover, study with antioxidant inhibitors confirmed the anti-apoptotic role of HO1 by which it played a decisive role in the development of HCC. PI fluorescence indicated 5.9 fold increase in the number of necrotic cells against control after carcinogenic exposure. Data probably indicated the regulatory role of necrosis in the progressive development of HCC in the DEN + CCl4 exposed mice. Post treatment of SAC, berberine and combined drug also increased necrotic effect with respect to carcinogen exposed group. Although the effect was minute in comparison with apoptotic role in the amelioration of DEN + CCl4 induced HCC.

The balance between cell proliferation and apoptosis is essential for the development and structural-functional maintenance of normal organs. The occurrence of cancer is supposedly due to the smother of normal apoptosis process, which caused the imbalance between cell proliferation and apoptosis [100,101]. In fact apoptosis constitutes an innate tissue defense against carcinogens by preventing survival of genetically damaged cells. As a result block of apoptosis has been elucidated as prevailing mechanism of liver tumor promotion in many rodent studies [102,103].

During the last decade, a considerable amount of research has been focused on cancer cell apoptosis. An effective way to augment anticancer strategies by using the developing knowledge of apoptosis could provide more targeted anti-tumor therapy for HCC [104]. Thus, here the role of apoptosis was assessed in the SAC and berberine mediated amelioration of DEN + CCl4 induced hepatocarcinoma.

In addition histological studies displayed anisonucleosis and dysplastic hepatocytes indicating the development of hepatocarcinoma after DEN + CCl4 exposure. Identification of distinct apoptotic cells by tunel and histological analysis after 30 days of SAC + berberine post treatment further suggested their participation in the induction of cell death. In commensurate to our experimental observations, co-treatment presented normal tissue structure which was marked by low scoring of dysplastic cells in the tissue section.

Continuation of the post treatment for another 30 days with a gap of 10 days of drug treatment probably introduced newer cells which in absence of carcinogen showed almost analogous to the control CYP2E1 activity alongside a reducing cellular microenvironment with an active anti-oxidant configuration. In the absence of oxidative stress Nrf2/HO1 revealed similar activities in comparison to control. Anti apoptotic Bcl2, $Bclx_L$, pro-apoptotic Bax, Bak, PUMA and tumor suppressor protein p53 expression also became like normal. Maintenance of JNK and PP2A activity within customary range retained Bcl2 phosphorylation in its basal level that resulted in similar type of Bcl2/Bax interaction as displayed in the control mice. In the absence of carcinogen, Akt only showed its regular activity and Mdm2-HDAC1 mediated p53 degradation was inhibited. In accordance with such events there was probably no nuclear translocation of p53 resulting no more activation of Bax. Mitochondrial membrane potential and MPT pore opening were similar to control resulting inhibition of cytochrome C release and maintained caspase3 at its standard activity. Reduced exposure of PS on the cell surface in association with the decrease in number of dysplastic hepatocytes in the tissue section indicated replacement of newer cells by the SAC and berberine after 60 days of treatment in DEN + CCl4 exposed mice.

To further substantiate the role of SAC and berberine in the amelioration of DEN + CCl4 induced HCC, we treated the animals with α-tocopherol, a potential antioxidant; Akt inhibitor triciribine and HDAC1 inhibitor trichostatin A. Treatment in combination with α-tocopherol, triciribine and trichostatin A or even with triciribine and trichostatin A able to reduce PCNA expression effectively in association with the decrease in dysplastic to normal cell ratio after 60 days of post treatment with the gap for 10 days in which no more treatment had been offered. Result was comparable to SAC + berberine treatment, suggesting that HDAC1 inhibitor SAC in association with berberine acted as Akt inhibitor and participated in the useful reduction of chemically induced hepatocarcinoma.

In conclusion, this study elucidated that bioactivation of DEN and CCl4 by CYP2E1 generated oxidative stress resulting Nrf2-HO1 dependent over expression of Bcl2 which was effectually phosphorylated at Ser70 by activated JNK and regulated Bcl2/Bax heterodimerization. Activated DEN + CCl4 further induced Akt dependent pMDM2-HDAC1 mediated p53 deacetylation leading to degradation of the protein, the possible reason of the reduction in Bax concentration. p53, Bax diminution and simultaneous accumulation of Ser70 phosphorylated Bcl2 were associated with cell proliferation and development of HCC in DEN + CCl4 exposed mice.

Effectual treatment with SAC + berberine indicated reduction in CYP2E1 mediated accumulation of ROS while Nrf2/HO1 activity and Bcl2 expression somehow maintained in the treated group. Drug mediated inhibition of JNK and PP2A activation reduced Bcl2/Bax interaction by dephosphorylating the Bcl2 in the treated group. Furthermore, inhibition of Akt protected p53 from its degradation by inhibiting the interaction between pMDM2 and HDAC1 within the nucleus after SAC + berberine treatment. As a result pro-apoptotic protein Bax was accumulated and that eventually directed the cell fate towards death. Continuation of the treatment demonstrated recovering of normal tissue structure in absence of bioactive carcinogen dependent compensatory cell proliferation. Finally this study provided evidences towards the efficacy of SAC and berberine treatment in the amelioration of DEN + CCl4 induced hepatocarcinoma in mice and suggests that they can be considered for wide range of therapeutic interventions of liver cancer or other solid tumors in the near future.

References

[1] W.Y. Lau, E.C.H. Lai, Hepatocellular carcinoma: current management and recent advances, Hepatobiliary Pancreat. Dis. Int. 7 (2008) 237–257.
[2] S. Caldwell, S.H. Park, The epidemiology of hepatocellular cancer: from the perspectives of public health problem to tumour biology, J. Gastroenterol. 44 (2009) 96–101.
[3] A.A. Oyagbemi, O.I. Azeez, A.B. Saba, Hepatocellular carcinoma and the underlying mechanisms, Afr. Health Sci. 10 (2010) 93–98.
[4] H. Nakagawa, S. Maeda, Molecular mechanisms of liver injury and hepatocarcinogenesis: focusing on the role of stress-activated MAPK, Pathol. Res. Int. 2012 (2012) 1–14.

[5] C.D. Mann, C.P. Neal, G. Garcea, M.M. Manson, A.R. Dennison, D.P. Berry, Phytochemicals as potential chemopreventive and chemotherapeutic agents in hepatocarcinogenesis, Eur. J. Cancer Prev. 18 (2009) 13–25.
[6] S.S. Lo, L.A. Dawson, E.Y. Kim, N.M. Mayr, J.Z. Wang, Z. Huang, H.R. Cardenes, Stereotactic body radiation therapy for hepatocellular carcinoma, Discov. Med. 9 (2010) 404–410.
[7] L.A. Dawson, C. Guha, Hepatocellular carcinoma: radiation therapy, Cancer J. 14 (2008) 111–116.
[8] J.J.G. Marin, B. Castano, P. Martinez-Becerra, R. Rosales, M.J. Monte, Chemotherapy in the treatment of primary liver tumours, Cancer Ther. 6 (2008) 711–728.
[9] S. Okada, Cancer chemoprevention as adjuvant therapy for hepatocellular carcinoma, Jpn. J. Clin. Oncol. 31 (2001) 357–358.
[10] C.W.L. Chua, S.P. Choo, Targeted therapy in hepatocellular carcinoma, Int. J. Hepatol. 2011 (2011) 1–11.
[11] H. Sun, H. Hou, P. Lu, L. Zhang, F. Zhao, C. Ge, T. Wang, M. Yao, J. Li, Isocorydine inhibits cell proliferation in hepatocellular carcinoma cell lines by inducing G2/M cell cycle arrest and apoptosis, PLoS One 7 (2012) e36808, http://dx.doi.org/10.1371/journal.pone.0036808.
[12] X.L. Guo, D. Li, F. Hu, J.R. Song, S.S. Zhang, W.J. Deng, K. Sun, Q.D. Zhao, X.Q. Xie, Y.J. Song, M.C. Wu, L.X. Wei, Targeting autophagy potentiates chemotherapy-induced apoptosis and proliferation inhibition in hepatocarcinoma cells, Cancer Lett. 320 (2012) 171–179.
[13] S.H. Park, Y. Lee, S.H. Han, S.Y. Kwon, O.S. Kwon, S.S. Kim, J.H. Kim, Y.H. Park, J.N. Lee, S.M. Bang, E.K. Cho, D.B. Shin, J.H. Lee, Systemic chemotherapy with doxorubicin, cisplatin and capecitabine for metastatic hepatocellular carcinoma, BMC Cancer 6 (2006) 1471–1476.
[14] L. Rossi, F. Zoratto, A. Papa, F. Iodice, M. Minozzi, L. Frati, S. Tomao, Current approach in the treatment of hepatocellular carcinoma, World J. Gastrointest. Oncol. 2 (2010) 348–359.
[15] H. Ueda, H. Fukuchi, C. Tanaka, Toxicity and efficacy of hepatic arterial infusion chemotherapy for advanced hepatocellular carcinoma, Oncol. Lett. 3 (2012) 259–263.
[16] F. Korangy, B. Höchst, M.P. Manns, T.F. Greten, Immunotherapy of hepatocellular carcinoma, Expert Rev. Gastroenterol. Hepatol. 4 (2010) 345–353.
[17] S. Díez, G. Navarro, C.T. de ILarduya, *In vivo* targeted gene delivery by cationic nanoparticles for treatment of hepatocellular carcinoma, J. Gene Med. 11 (2009) 38–45.
[18] M.P. Radosavljevic, Hepatocellular carcinoma: the place of new medical therapies, Ther. Adv. Gastroenterol. 3 (2010) 259–267.
[19] J.M. Llovet, J. Bruix, Molecular targeted therapies in hepatocellular carcinoma, Hepatology 48 (2008) 1312–1327.
[20] Y.F. Liu, B.S. Zha, H.L. Zhang, X.J. Zhu, Y.H. Li, J. Zhu, X.H. Guan, Z.Q. Feng, J.P. Zhang, Characteristic gene expression profiles in the progression from liver cirrhosis to carcinoma induced by diethylnitrosamine in a rat model, J. Exp. Clin. Cancer Res. 28 (2009) 107–123.
[21] S. Sundaresan, P. Subramanian, S-allylcysteine inhibits circulatory lipid peroxidation and promotes antioxidants in N-nitrosodiethylamine-induced carcinogenesis, Pol. J. Pharmacol. 55 (2003) 37–42.
[22] S. Sundaresan, P. Subramanian, Prevention of N-nitrosodiethylamine-induced hepatocarcinogenesis by S-allylcysteine, Mol. Cell. Biochem. 310 (2008) 209–214.
[23] X. Zhao, J.J. Zhang, X. Wang, X.Y. Bu, Q. Lou, G.L. Zhang, Effect of berberine on hepatocyte proliferation, inducible nitric oxide synthase expression, cytochrome P450 2E1 and 1A2 activities in diethylnitrosamine- and phenobarbital-treated rats, Biomed. Pharmacother. 62 (2008) 567–572.
[24] J. Wongbutdee, Physiological effects of berberine, Thai Pharm. Health Sci. J. 4 (2008) 78–83.
[25] P.O. Seglen, Preparation of isolated rat liver cells, Methods Cell Biol. 13 (1976) 29–83.
[26] P. Inarrea, H. Moini, D. Han, D. Rettori, I. Aguilo, M.A. Alava, M. Iturralde, E. Cadenas, Mitochondrial respiratory chain and thioredoxin reductase regulate intermembrane Cu, Zn-superoxide dismutase activity: implications for mitochondrial energy metabolism and apoptosis, Biochem. J. 405 (2007) 173–179.
[27] P.X. Petit, M. Goubern, P. Diolez, S.A. Susin, N. Zamzami, G. Kroemer, Disruption of the outer mitochondrial membrane as a result of large amplitude swelling: the impact of irreversible permeability transition, FEBS Lett. 426 (1998) 111–116.
[28] J.D. Dignam, R.M. Lebovitz, R.G. Roeder, Accurate transcription initiation by RNA polymerase II in a soluble extract from isolated mammalian nuclei, Nucleic Acids Res. 11 (1983) 1475–1489.
[29] C. Domenicotti, D. Paola, A. Vitali, M. Nitti, D. Cottalasso, E. Melloni, G. Poli, U.M. Marinari, M.A. Pronzato, Mechanisms of inactivation of hepatocyte protein kinase C isoforms following acute ethanol treatment, Free Radic. Biol. Med. 25 (1998) 529–535.
[30] T.K. Chang, C.L. Crespi, D.J. Waxman, Spectrophotometric analysis of human CYP2E1-catalyzed p-nitrophenol hydroxylation, Methods Mol. Biol. 320 (2006) 127–131.
[31] J.D. Kim, R.J.M. McCarter, B.P. Yu, Influence of age, exercise, and dietary restriction on oxidative stress in rats, Aging Clin. Exp. Res. 8 (1996) 123–129.
[32] W. Stratford May, P.G. Tyler, T. Ito, D.K. Armstrong, K.A. Qatsha, N.E. Davidson, Interleukin-3 and bryostatin-1 mediate hyperphosphorylation of BCL2α in association with suppression of apoptosis, J. Biol. Chem. 269 (1994) 26665–26870.
[33] M.R.M. Harrison, A.S. Georgiou, H.P. Spaink, V.T. Cunliffe, The epigenetic regulator histone deacetylase1 promotes transcription of a core neurogenic programme in zebrafish embryos, BMC Genomics 12 (2011) 24–41.
[34] C. Caron, C.P. Pajot, L.A. van Grunsven, E. Col, C. Lestrat, S. Rousseaux, S. Khochbin, Cdyl: a new transcriptional co-repressor, EMBO Rep. 4 (2003) 877–882.
[35] M.J. Marinissen, T. Tanos, M. Bolo, M.R. de Sagarra, O.A. Coso, A. Cuadrado, Inhibition of heme oxygenase-1 interferes with the transforming activity of the Kaposi sarcoma herpes virus encoded G protein-coupled receptor, J. Biol. Chem. 281 (2006) 11332–11346.
[36] K.F. Chen, P.Y. Yeh, C. Hsu, C.H. Hsu, Y.S. Lu, H.P. Hsieh, P.J. Chen, A.L. Cheng, Bortezomib overcomes tumour necrosis factor-related apoptosis-inducing ligand resistance in hepatocellular carcinoma cells in part through the inhibition of the phosphatidylinositol 3-kinase/akt pathway, J. Biol. Chem. 284 (2009) 11121–11133.
[37] A.S. Burke, L.A. MacMillan-Crow, J.A. Hinson, Reactive nitrogen species in acetaminophen-induced mitochondrial damage and toxicity in mouse hepatocytes, Chem. Res. Toxicol. 23 (2010) 1286–1292.
[38] A. Bernareggi, Clinical pharmacokinetics of nimesulide, Clin. Pharmacokinet. 35 (1998) 247–274.
[39] R. Schlatter, K. Schmich, A. Lutz, J. Trefzger, O. Sawodny, M. Ederer, I. Merfort, Modeling the TNFα-induced apoptosis pathway in hepatocytes, PLoS One 6 (2011) e18646–e18661.
[40] L. Huerta, L. Rancan, C. Simón, J. Isea, E. Vidaurre, E. Vara, I. Garuttic, F.G. Aragoneses, Ischaemic preconditioning prevents the liver inflammatory response to lung ischaemia/reperfusion in a swine lung autotransplant model, Eur. J. Cardiothorac. Surg. (2012), http://dx.doi.org/10.1093/ejcts/ezs599.
[41] M.R. Cheng, Q. Li, T. Wan, B. He, J. Han, H.X. Chen, F.X. Yang, W. Wang, H.Z. Xu, T. Ye, B.B. Zha, Galactosylated chitosan/5-fluorouracil nanoparticles inhibit mouse hepatic cancer growth and its side effects, World J. Gastroenterol. 18 (2012) 6076–6087.
[42] W.F. Khalaf, H. White, M.J. Wenning, A. Orazi, R. Kapur, D.A. Ingram, *K-Ras* is essential for normal fetal liver erythropoiesis, Blood 105 (2005) 3538–3541.
[43] D.N. Roy, S. Mandal, G. Sen, S. Mukhopadhyay, T. Biswas, 14-Deoxyandrographolide desensitizes hepatocytes to tumour necrosis factor-alpha-induced apoptosis through calcium-dependent tumour necrosis factor receptor superfamily member 1A release via the NO/cGMP pathway, Br. J. Pharmacol. 160 (2010) 1823–1843.
[44] H. Tateossian, R.E. Hardisty-Hughes, S. Morse, M.R. Romero, H. Hilton, C. Dean, S.D. Brown, Regulation of TGF-beta signalling by Fbxo11, the gene mutated in the *Jeff otitis* media mouse mutant, Pathogenetics 2 (2009) 5–19.
[45] T. Hussain, H.H. Siddiqui, S. Fareed, M. Vijayakumar, C.V. Rao, Evaluation of chemopreventive effect of *Fumaria indica* against N-nitrosodiethylamine and CCl_4-induced hepatocellular carcinoma in Wistar rats, Asian Pac. J. Trop. Med. 5 (2012) 623–629.
[46] M. Joo, Y.K. Kang, M.R. Kim, H.K. Lee, J.J. Jang, Cyclin D1 overexpression in hepatocellular carcinoma, Liver 21 (2001) 89–95.
[47] P. Parekh, K.V. Rao, Overexpression of cyclin D1 is associated with elevated levels of MAP kinases, Akt and Pak1 during diethylnitrosamine-induced progressive liver carcinogenesis, Cell Biol. Int. 31 (2007) 35–43.
[48] L.X. Qin, Z.Y. Tang, The prognostic molecular markers in hepatocellular carcinoma, World J. Gastroenterol. 8 (2002) 385–392.
[49] H. Yamazaki, Y. Oda, Y. Funae, Participation of rat liver cytochrome P450 2E1 in the activation of N-nitrosodimethylamine and N-nitrosodiethylamine to products genotoxic in an acetyltransferase-overexpressing *Salmonella typhimurium* strain, Carcinogenesis 13 (1992) 979–985.
[50] M. Kujawska, E. Ignatowicz, M. Murias, M. Ewertowska, K. Mikołajczyk, J. Jodynis-liebert, Protective effect of red beetroot against carbon tetrachloride- and N-Nitrosodiethylamine-induced oxidative stress in rats, J. Agric. Food Chem. 57 (2009) 2570–2575.
[51] K.W. Kang, S.J. Lee, S.G. Kim, Molecular mechanism of Nrf2 activation by oxidative stress, Antioxid. Redox Signal. 7 (2005) 1664–1673.
[52] N. Weis, A. Weigert, A. von Knethen, B. Brune, Heme oxygenase-1 contributes to an alternative macrophage activation profile induced by apoptotic cell supernatants, Mol. Biol. Cell. 20 (2009) 1280–1288.
[53] X. Deng, P. Ruvolo, B. Carr, W.S. May Jr., Survival function of ERK1y2 as IL-3-activated, staurosporine-resistant Bcl2 kinases, Proc. Natl. Acad. Sci. U. S. A. 97 (2000) 1578–1583.
[54] V. Graupner, E. Alexander, T. Overkamp, O. Rothfuss, V. De Laurenzi, B.F. Gillissen, P.T. Daniel, K. Schulze-Osthoff, F. Essmann, Differential regulation of the proapoptotic multidomain protein Bak by p53 and p73 at the promoter level, Cell Death Differ. 18 (2011) 1130–1139.
[55] W. Qiu, X. Wang, B. Leibowitz, W. Yang, L. Zhang, J. Yu, PUMA-mediated apoptosis drives chemical hepatocarcinogenesis in mice, Hepatology 54 (2011) 1249–1258.
[56] A. Insinga, S. Monestiroli, S. Ronzoni, R. Carbone, M. Pearson, G. Pruneri, G. Viale, E. Appella, P.G. Pelicci, S. Minucci, Impairment of p53 acetylation, stability and function by an oncogenic transcription factor, EMBO J. 23 (2004) 1144–1154.
[57] A. Ito, Y. Kawaguchi, C.H. Lai, J.J. Kovacs, Y. Higashimoto, E. Appella, T. Yao, MDM2–HDAC1-mediated deacetylation of p53 is required for its degradation, EMBO J. 21 (2002) 6236–6245.
[58] Y. Ogawara, S. Kishishita, T. Obata, Y. Isazawa, T. Suzuki, K. Tanaka, N. Masuyama, Y. Gotoh, Akt enhances Mdm2-mediated ubiquitination and degradation of p53, J. Biol. Chem. 277 (2002) 21843–21850.
[59] Y. Wang, Y.A. Suh, M.Y. Fuller, J.G. Jackson, S. Xiong, T. Terzian, A.Q. Cardama, J.A. Bankson, A.K. El-Naggar, G. Lozano, Restoring expression of wild-type p53 suppresses tumour growth but does not cause tumour regression in mice with a p53 missense mutation, J. Clin. Invest. 121 (2011) 893–904.
[60] J.H. Mowatt, C. Dive, J.C. Martinou, D. James, Role of mitochondrial membrane permeabilization in apoptosis and cancer, Oncogene 23 (2004) 2850–2860.
[61] H. Higuchi, M. Adachi, S. Miura, G.J. Gores, H. Ishii, The mitochondrial permeability transition contributes to acute ethanol-induced apoptosis in rat hepatocytes, Hepatology 34 (2001) 320–328.
[62] D.E. Pritchard, J. Singh, D.L. Carlisle, S.R. Patierno, Cyclosporin A inhibits chromium (VI) induced apoptosis and mitochondrial cytochrome c release and restores clonogenic survival in CHO cells, Carcinogenesis 21 (2000) 2027–2033.

[63] A.I. Vogel, Practical Organic Chemistry, 3rd ed. Pearson Education, India, 1962.
[64] J.K. Lin, Nitrosamines as potential environmental carcinogens in man, Clin. Biochem. 23 (1990) 67–71.
[65] P. Jakszyn, A. Agudo, R. Ibáñez, R.G. Closas, G. Pera, P. Amiano, C.A. González, Development of a food database of nitrosamines, heterocyclic amines, and polycyclic aromatic hydrocarbons, J. Nutr. 134 (2004) 2011–2014.
[66] V. Sharma, M. Singh, N-Nitrosodimethyl amine as a hazardous chemical toxicant in drinking water, Int. Res. J. Pharm. 3 (2012) 60–65.
[67] S.E. Chuang, M.L. Kuo, C.H. Hsu, C.R. Chen, J.K. Lin, G.M. Lai, C.Y. Hsieh, A.L. Cheng, Curcumin-containing diet inhibits diethylnitrosamine-induced murine hepatocarcinogenesis, Carcinogenesis 21 (2000) 331–335.
[68] R. Peto, R. Gray, P. Brantom, P. Grasso, Dose and time relationships for tumour induction in the liver and oesophagus of 4080 inbred rats by chronic ingestion of N-nitrosodiethylamine or N-nitrosodimethylamine, Cancer Res. 51 (1991) 6452–6469.
[69] W. Qiu, X. Wang, B. Leibowitz, W. Yang, L. Zhang, J. Yu, PUMA-mediated apoptosis drives chemical hepatocarcinogenesis in mice, Hepatology 54 (2011) 1249–1258.
[70] T. Sakurai, S. Maeda, L. Chang, M. Karin, Loss of hepatic NF-kappa B activity enhances chemical hepatocarcinogenesis through sustained c-Jun N-terminal kinase 1 activation, Proc. Natl. Acad. Sci. U. S. A. 103 (2006) 10544–10551.
[71] T. Hussain, H.H. Siddiqui, S. Fareed, M. Vijayakumar, C.V. Rao, Evaluation of chemopreventive effect of *Fumaria indica* against N-nitrosodiethylamine and CCl_4-induced hepatocellular carcinoma in Wistar rats, Asian Pac. J. Trop. Med. 5 (2012) 623–629.
[72] E. Pikarsky, R.M. Porat, I. Stein, R. Abramovitch, S. Amit, S. Kasem, E. Gutkovich-Pyest, S. Urieli-Shoval, E. Galun, Y. Ben-Neriah, NF-kappaB functions as a tumour promoter in inflammation-associated cancer, Nature 431 (2004) 461–466.
[73] N.M. Abdel-Hamid, M.A. Fawzy, M.A. El-Moselhy, Evaluation of hepatoprotective and anticancer properties of aqueous olive leaf extract in chemically induced hepatocellular carcinoma in rats, Am. J. Med. Med. Sci. 1 (2011) 15–22.
[74] N. Sokkar, O. El-Gindi, S. Sayed, S. Mohamed, Z. Ali, I. Alfishawy, Antioxidant, anticancer and hepatoprotective activities of *Cotoneaster horizontalis* Decne extract as well as α-tocopherol and amygdalin production from *in vitro* culture, Acta Physiol. Plant, http://dx.doi.org/10.1007/s11738-013-1276-z.
[75] S. De, S. De, *Gymnosporia montana*, a potential hepatoprotective and anticancer drug-an overview, Asian J. Pharm. Clin. Res. 5 (2012) 20–24.
[76] M.J. Wu, C.Y. Weng, H.Y. Ding, P.J. Wu, Anti-inflammatory and antiviral effects of *Glossogyne tenuifolia*, Life Sci. 76 (2005) 1135–1146.
[77] X.H. Tang, J. Gao, Y.P. Wang, L.Z. Xu, X.N. Zhao, Q. Xu, Hepatoprotective effects of chloroform extract from leaf of *Terminalia catappa* in relation to the inhibition of liver IL-6 expression, Zhongguo Zhong Yao Za Zhi 28 (2003) 1170–1174.
[78] B. Sun, M. Karin, NF-kappaB signaling, liver disease and hepatoprotective agents, Oncogene 27 (2008) 6228–6244.
[79] S.E. Chuang, M.L. Kuo, C.H. Hsu, C.R. Chen, J.K. Lin, G.M. Lai, C.Y. Hsieh, A.L. Cheng, Curcumin-containing diet inhibits diethylnitrosamine-induced murine hepatocarcinogenesis, Carcinogenesis 21 (2000) 331–335.
[80] M.N.T. Attia, M.A. Ali, Hepatoprotective activity of allicin against carbon tetrachloride induced hepatic injury in rats, J. Biol. Sci. 6 (2006) 457–468.
[81] H. Amagase, Clarifying the real bioactive constituents of garlic, J. Nutr. 136 (2006) 716–725.
[82] Y. Sun, K. Xun, Y. Wang, X. Chen, A systematic review of the anticancer properties of berberine, a natural product from Chinese herbs, Anticancer Drugs 20 (2009) 757–769.
[83] N. Tong, J. Zhang, Y. Chen, Z. Li, Y. Luo, H. Zuo, X. Zhao, Berberine sensitizes mutliple human cancer cells to the anticancer effects of doxorubicin *in vitro*, Oncol. Lett. 3 (2012) 1263–1267.
[84] A. Ravid, R. Korean, The role of reactive oxygen species in the anticancer activity of vitamin D, Anticancer. Res. 164 (2003) 357–367.
[85] R.O. Recknagel, E.A. Glende Jr., Carbon tetrachloride hepatotoxicity-an example of lethal cleavage, CRC Crit. Rev. Toxicol. 2 (1973) 263–297.
[86] S.S. Al-Rejaie, A.M. Aleisa, A.A. Al-Yahya, S.A. Bakheet, A. Alsheikh, A.G. Fatani, O.A. Al-Shabanah, M.M. Sayed-Ahmed, Progression of diethylnitrosamine-induced hepatic carcinogenesis in carnitine-depleted rats, World J. Gastroenterol. 15 (2009) 1373–1380.
[87] K.L. Cheung, S. Yu, Z. Pan, J. Ma, T.Y. Wu, A.N.T. Kong, tBHQ-Induced HO-1 expression is mediated by calcium through regulation of Nrf2 binding to enhancer and polymerase II to promoter region of HO-1, Chem. Res. Toxicol. 24 (2011) 670–676.
[88] S. Kongpetch, V. Kukongviriyapan, A. Prawan, L. Senggunprai, U. Kukongviriyapan, B. Buranrat, Crucial role of heme oxygenase-1 on the sensitivity of cholangiocarcinoma cells to chemotherapeutic agents, PLoS One 7 (2012) e34994, http://dx.doi.org/10.1371/journal.pone.0034994.
[89] C.R.P. Kruel, L.F.R. Pinto, T.C.M. Blanco, T.C. Barja-Fidalgo, L.L. Melo, C.D.P. Kruel, Evaluation of the heme oxygenase-1 expression in esophagitis and esophageal cancer induced by different reflux experimental models and diethylnitrosamine, Acta Cir. Bras. 25 (2010) 304–310.
[90] J. Dulak, A. Józkowicz, Carbon monoxide—a "new" gaseous modulator of gene expression, Acta. Biochim. Pol. 50 (2003) 31–47.
[91] J. Cao, G. Drummond, K. Inoue, K. Sodhi, X.Y. Li, S. Omura, Upregulation of heme oxygenase-1 combined with increased adiponectin lowers blood pressure in diabetic spontaneously hypertensive rats through a reduction in endothelial cell dysfunction, apoptosis and oxidative stress, Int. J. Mol. Sci. 9 (2008) 2388–2406.
[92] Z.N. Oltvai, C.L. Milliman, S.J. Korsmeyer, Bcl-2 heterodimerizes *in vivo* with a conserved homolog, Bax that accelerates programmed cell death, Cell 74 (1993) 609–619.
[93] L. Hui, K. Zatloukal, H. Scheuch, E. Stepniak, E.F. Wagner, Proliferation of human HCC cells and chemically induced mouse liver cancers requires JNK1-dependent p21 downregulation, J. Clin. Invest. 118 (2008) 3943–3953.
[94] H. Nagata, E. Hatano, M. Tada, M. Murata, K. Kitamura, H. Asechi, M. Narita, A. Yanagida, N. Tamaki, S. Yagi, I. Ikai, K. Matsuzaki, S. Uemoto, Inhibition of c-Jun NH2-terminal kinase switches Smad3 signaling from oncogenesis to tumour-suppression in rat hepatocellular carcinoma, Hepatology 49 (2009) 1944–1953.
[95] E.H. Xiao, J.Q. Li, J.F. Huang, Effects of p53 on apoptosis and proliferation of hepatocellular carcinoma cells treated with transcatheter arterial chemoembolization, World J. Gastroenterol. 10 (2004) 190–194.
[96] V. Solozobova, A. Rolletschek, C. Blattner, Nuclear accumulation and activation of p53 in embryonic stem cells after DNA damage, BMC Cell Biol. 10 (2009) 46–56.
[97] L. Chen, C. Shao, E. Cobos, J.S. Wang, W. Gao, 1,4-(Methylnitro-Samino)-1-(3-Pyridyl)-1-Butanone induces CRM1-dependent p53 nuclear accumulation in human bronchial epithelial cells, Toxicol. Sci. 116 (2010) 206–215.
[98] I. Silins, N. Finnberg, A. Stahl, J. Hogberg, U. Stenius, Reduced ATM kinase activity and an attenuated p53 response to DNA damage in carcinogen-induced preneoplastic hepatic lesions in the rat, Carcinogenesis 22 (2001) 2023–2031.
[99] G. Kroemer, J.C. Reed, Mitochondrial control of cell death, Nat. Med. 6 (2000) 513–519.
[100] S. Kanzler, P.R. Galle, Apoptosis and the liver, Semin. Cancer Biol. 10 (2000) 173–184.
[101] Y.N. Park, K.J. Chae, Y.B. Kim, C. Park, N. Theise, Apoptosis and proliferation in hepatocarcinogenesis related to cirrhosis, Cancer 92 (2001) 2733–2738.
[102] W. Bursch, B. Grasl-Kraupp, U. Wastl, K. Hufnagl, M. Chabicovsky, H. Taper, R. Schulte-Hermann, Role of apoptosis for mouse liver growth regulation and tumour promotion: comparative analysis of mice with high (C3H/He) and low (C57Bl/6 J) cancer susceptibility, Toxicol. Lett. 149 (2004) 25–35.
[103] Y. Li, L. Chen, T.H. Chan, M. Liu, K.L. Kong, J.L. Qiu, Y. Li, Y.F. Yuan, X.Y. Guan, SPOCK1 is regulated by CHD1L and blocks apoptosis and promotes HCC cell invasiveness and metastasis in mice, Gastroenterology 144 (2013) 179–191.
[104] H. Nakagawa, Y. Hirata, K. Takeda, Y. Hayakawa, T. Sato, H. Kinoshita, K. Sakamoto, W. Nakata, Y. Hikiba, M. Omata, H. Yoshida, K. Koike, H. Ichijo, S. Maeda, Apoptosis signal-regulating kinase 1 inhibits hepatocarcinogenesis by controlling the tumour-suppressing function of stress-activated mitogen-activated protein kinase, Hepatology 54 (2011) 185–195.